Marine Geology 411 (2019) 62–77

Contents lists available at ScienceDirect

Marine Geology

journal homepage: www.elsevier.com/locate/margo

The origin and dynamics of coastal boulders in a semi-enclosed shallow basin: A northern Adriatic case study

Sara Biolchi[a,*], Stefano Furlani[a], Stefano Devoto[a], Giovanni Scicchitano[b], Tvrtko Korbar[c], Ivica Vilibić[d], Jadranka Šepić[d]

[a] Department of Mathematics and Geosciences, University of Trieste, Trieste, Italy
[b] Studio Geologi Associati T.S.T., Catania, Italy
[c] Croatian Geological Survey, Department of Geology, Zagreb, Croatia
[d] Institute of Oceanography and Fisheries, Split, Croatia

ARTICLE INFO

Editor: Edward Anthony

ABSTRACT

This paper documents the analysis of a coastal boulder deposit that was recently identified along the northern Adriatic coast (Premantura Promontory, Istria, Croatia). Accumulations of large boulders have not previously been reported in the northern Adriatic, which can be viewed as a semi-enclosed basin. A multidisciplinary approach was used to investigate the site including geological and geomorphological surveys, together with the use of an Unmanned Aerial Vehicle (UAV), digital photogrammetric analysis, hydrodynamic modelling and ^{14}C AMS datings. Measurements of boulder position, elevation, size, shape and density were fed into hydrodynamic equations that are used to estimate the minimum storm and tsunami wave height required to enable the accumulation of boulders. Biogenic marine carbonate encrustations observed on 14 boulders suggest the infra- and sublittoral zones as source areas, while for most of the boulders a subaerial origin is hypothesised. The boulder deposit occurs on a flat promontory where the topography, together with the stratified limestone bedding planes and dense joint pattern constitute the predisposing factors for boulder size and detachment. Comparisons between satellite images taken between 2008 and 2017, pictures collected from Internet and a 2012 snorkel survey of the Istrian coast made it possible to highlight the emplacement of a boulder with an estimated weight of 7.65 t during late 2013 or early 2014. The study examines the mechanisms that may be responsible for the detachment and transport of these large limestone rock fragments from the emergent part of the coast and from the sea bed towards inland areas. The results suggest the occurrence of very recent extreme weather conditions as well as multiple historical storm events and exclude a tsunami origin of the boulders.

1. Introduction

Coastal environments are highly dynamic and can be affected by significant morphological changes in very short spaces of time as a result of the interaction between waves, tides and fluvial inputs, which in turn are conditioned by relative sea-level changes, climatic settings and neotectonic processes (Pethick, 1984). In particular, rapid modifications of the coastal environment are caused by severe events acting over timescales ranging from seconds (waves) to hours (tsunamis and storm surges). Such events are able to generate a complex sedimentary record that has significant morphological features, especially on rocky coasts where the strength of the waves can lead to the accumulation of very impressive boulders, in terms of size and weight (Morton et al., 2011).

Although boulder deposits are very common along ocean coasts (i.e., Hearty, 1997; Williams and Hall, 2004; Etienne and Paris, 2010; Switzer and Burston, 2010; Fichaut and Suanez, 2011; Autret et al., 2016; Engel et al., 2016; Lau et al., 2016; Hearty and Tormey, 2017; Soria et al., 2018) and in the Mediterranean Sea, (Mastronuzzi et al., 2006; Furlani et al., 2014a), they are rare along the coast of the Adriatic Sea. The latter is a semi-enclosed and relatively shallow basin, where boulder deposits have only been reported along the coasts of Apulia close to the Ionian Sea (Mastronuzzi and Sansò, 2004). In particular, this is first time that boulder deposits have been found in the north-eastern Adriatic Sea, along the Croatian coast.

It has been documented that forces strong enough to detach boulders from the ground and transport them ashore can be generated both by waves associated with storm events and by major tsunami

* Corresponding author.
E-mail address: sbiolchi@units.it (S. Biolchi).

https://doi.org/10.1016/j.margeo.2019.01.008
Received 21 March 2018; Received in revised form 22 January 2019; Accepted 23 January 2019
Available online 16 February 2019
0025-3227/

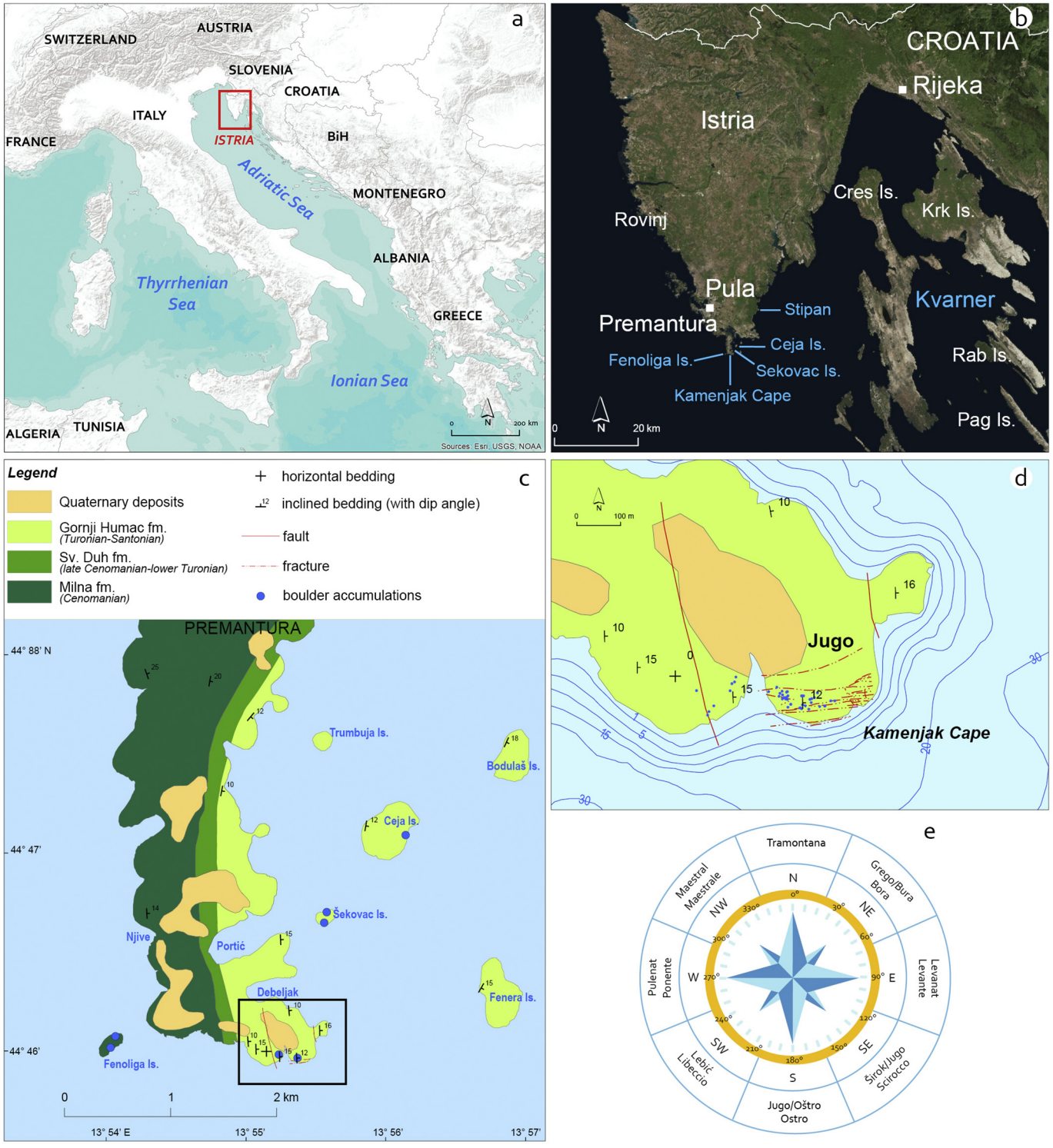

Fig. 1. a) Geographical setting of the study area in the northeastern Adriatic Sea (central Mediterranean basin); b) location of the boulder deposits; c) simplified geological map of the southernmost Istria (modified after Polšak, 1967); d) detail geological map of the Kamenjak Cape; e) wind rose of the Adriatic Sea (names of winds in Croatian and Italian languages). (For interpretation of the references to colour in this figure legend, the reader is referred to the web version of this article.)

events (Morton et al., 2011). Unfortunately, the marks of tsunamis in coastal sediments are very difficult to distinguish from those of violent storm surges as both are high-energy marine events that result in similar deposits (Rodríguez-Ramírez et al., 2016; Soria et al., 2017). Some research criteria could be inferred from deposit features in that storm wave deposits tend to be wedge-shaped where sediments are transported by bed load, while tsunami deposits are sheet-shaped and characterised by suspended load. Moreover, tsunami deposits extend farther inland than their storm-generated counterparts as a result of long period waves with respect to the short wave periods encountered during storms (Morton et al., 2007; Goto et al., 2010).

Using the sizes and shapes of boulders surveyed along the coast, many authors have developed hydrodynamic equations to build models capable of recognising the origin of their deposits (Nott, 1997, 2003;

Noormets et al., 2004; Imamura et al., 2008; Pignatelli et al., 2009; Benner et al., 2010; Nandasena et al., 2011; Engel and May, 2012; Watanabe et al., 2016). These model estimates, ascribed to wind-generated waves, storm surges and tsunamis in a particular area, attempt to find the best match between the observed boulder dynamics and the forcing factors in the area. In general, the minimum storm-wave amplitude to dislodge a boulder of given size is larger than the required minimum tsunami-wave amplitude and the ratio between amplitudes is largest for large masses and large roughness values (Weiss and Diplas, 2015).

Hydrodynamic equations have been widely used by various authors to investigate the origin of past and recent boulder accumulations at several sites in the Mediterranean Sea (i.e., Mastronuzzi et al., 2007, Apulia, S Italy - tsunami; Scheffers and Scheffers, 2007, Crete Is., Greece - tsunami; Scicchitano et al., 2007, 2012, Barbano et al., 2010, Sicily - tsunami; Maouche et al., 2009, Algeria - tsunami; Reicherter and Becker-Heidmann, 2009, Almeria, S Spain - tsunami; for Malta Mottershead et al., 2014 – tsunami, Biolchi et al., 2016, Causon Deguara and Gauci, 2017 - storm events respectively; Vacchi et al., 2012, Lesbos Is., Greece - tsunami; Öğretmen et al., 2015, Silifke, S Turkey - tsunami; Raji et al., 2015, Morocco – storm events and tsunami; Shah-Hosseini et al., 2016, Egypt – storm events and tsunami; Piscitelli et al., 2017, Martigues, France – storm events; Roig-Munar et al., 2017, Menorca Is., Spain – tsunami; Pepe et al., 2018, Favignana Is., S Italy – storm events). Therefore, boulders have been widely used to infer tsunami deposition along Mediterranean coasts. By contrast, Williams and Hall (2004) have cautioned against these systematic tsunami attributions based on a study of “megaclast” accumulations produced by large storm surges on the Atlantic coast of Ireland. Despite the possible correlation with historical tsunamis, on the island of Malta, Biolchi et al. (2016) ascribed the deposition of the majority of boulders to severe storm waves by using a multidisciplinary approach that - together with the hydrodynamic modelling - also took into account local geomorphological and climatic conditions. Recently, Marriner et al. (2017) have analysed tsunami and storm data contained in the EM-DAT (Emergency Events Database) database for the period 1900–2015 and observed that storms are more than eight times deadlier and costlier than tsunamis and that up to 90% of tsunami attributions of high-energy events in the Mediterranean coastal record should be reconsidered.

However, these equations, although widely used, do not respond perfectly to the question “storm or tsunami?” since none of them takes into account all the geological and geomorphological features of the deposit simultaneously, such as the spatial arrangement of morphogenic zones, topographic irregularities and bed roughness, the distance from the coastline, the inland elevation, the elevation at which the boulders are detached etc. In this framework, Zainali and Weiss (2015) highlighted the shortcomings of the standard methods currently used and suggested that three-dimensional simulations, including variables such as angle of incident wave or heterogeneous mass distribution within the boulder, are needed to improve our understanding of boulder dislodgement. In addition, Naylor et al. (2016) have highlighted the importance of geomorphological control on boulder entrainment and transport as part of palaeo-storm and sedimentary reconstruction studies.

This work adds a new site for extreme wave deposit in the Mediterranean basin and aims to deepen the debate between a storm or tsunami genesis for these kinds of deposits. In particular, it aims to examine and discuss the mechanisms underlying the detachment, transport and accumulation of the large boulders recently found on the southernmost tip of the Istrian peninsula, in northwestern Croatia (Fig. 1a, b).

We adopted a multidisciplinary approach, which integrated geological and geomorphological surveys (both aerial and underwater), geomechanical investigations, aerial and terrestrial photogrammetry, hydrodynamic models and assessments of regional wave and tsunami climates.

2. Study area

2.1. Geology and geomorphology

The study area (Fig. 1) is located in the northernmost tip of the Mediterranean basin, along the Croatian coast of the Adriatic Sea. The boulder deposit is located in the southernmost sector of the Istrian peninsula, in the Premantura Promontory (that includes the Kamenjak Nature Park).

A few hundred metres thick succession of stratified Late Cretaceous carbonate rocks, deposited during the Cenomanian to Santonian stages (Vlahović et al., 2003) on top of the Adriatic carbonate platform (Vlahović et al., 2005; Korbar, 2009; Jurkovšek et al., 2016), crop out continuously along the promontory, dipping gently towards the East (Fig. 1c). Southern Istria belongs to the Eastern limb of a broad Istrian anticline probably formed during the late Cretaceous era (Matičec et al., 1996), and to the Adriatic foreland of the Dinarides (Korbar, 2009), which is characterised by tectonic subsidence during the Holocene (Antonioli et al., 2009; Surić et al., 2014).

The Kamenjak Nature Park, which covers two thirds of the long and narrow Premantura Promontory, is characterised by elevations up to 50 m above sea level, rounded bays, pocket beaches and small islands. The northwest coast is mainly characterised by plunging cliffs largely conditioned by the occurrence of vertical fractures and faults, which favour the development of sea caves, stacks and arches (Furlani et al., 2012). Conversely, the southern and eastern coasts are characterised by gentle slopes, which generally follow the dip angles of the strata. The southeasternmost tip of the Premantura Promontory is called Jugo, after the powerful southeasterly wind (*jugo* in Croatian). The southeasternmost point of the promontory – Cape Kamenjak – consists of a Turonian age shallow marine limestone succession (Fig. 1c). The latter alternates between thin-bedded (10–30 cm), fine-grained peloidal packstones, and thick-bedded (50–150 cm) mudstone through to wackestone containing algal oncoids and rare rudist bivalve lithosomes and algal oncoids, typical of the lower part of the Gornji Humac formation (Gušić and Jelaska, 1990).

2.2. Northern Adriatic wave, storm surge and tsunami climates

The northern Adriatic Sea is a semi-enclosed basin in the northern Mediterranean Sea, where winds and waves are strongly influenced by the orography. The dominant winds (Heimann, 2001) are the sirocco (*jugo* in Croatian), bora (*bura* in Croatian) and libeccio (Fig. 1e).

The sirocco blows from the southeast, thus having the largest fetch and potential for wave growth in the northern Adriatic. For this reason, the highest waves result from long-lasting siroccos blowing across much of the Adriatic (Smirčić et al., 1996), with significant and maximum wave heights of 5.3 m and 10.8 m, respectively, measured over a roughly 10-year interval (1978–1986) in locations about 50 km southwest of the Premantura Promontory. Locally, due to the orography of the Istrian peninsula, the sirocco is modulated to blow from the south and south-southeast, as seen on data from the Pula climatological station located not far from the Premantura Promontory.

The Bora is a strong, gusting katabatic wind which blows from the northeast, and is generated by a chain of mountains breaking a northeasterly flow of continental air masses (Grisogono and Belušić, 2009) sometimes persisting for a week or more (Mihanović et al., 2013). It generates significant waves along the western Adriatic coast, reaching its maximum force in the area around the Bay of Kvarner (Grisogono and Belušić, 2009), where its gustiness and occasional hurricane force wind speeds above 33 m/s create steep ocean waves and associated sea spray. In the area of the Premantura Promontory, the bora is much more frequent than the sirocco wind (Fig. 1).

The third dominant wind in the northern Adriatic is the libeccio which blows from the southwest. This is an impulsive wind, usually of much shorter duration than either the sirocco or bora and while its

frequency is not high in the area around the Premantura Promontory, the waves generated can prove considerable (Leder et al., 1998).

Stormy conditions with high waves predominate during the autumn and winter periods, between November and March (Pomaro et al., 2017). Locally, the Premantura Promontory is exposed to waves from both the open Adriatic and the Bay of Kvarner, where the bora can blow hard during extreme events (Grisogono and Belušić, 2009; Kuzmić et al., 2015), causing sea spray and short period waves over the limited fetch.

The same part of the year, from November to February, is characterised by the highest mean sea levels and storm surges (Vilibić, 2006), which can lead to the flooding of coastal regions such as nearby Venice (Carbognin et al., 2010). Together with the Adriatic seiche (Cerovečki et al., 1997) and tides, which are much larger than in the rest of the Mediterranean Sea (Tsimplis et al., 1995), extreme sea levels can reach 1.5 m above mean sea level (Međugorac et al., 2015; Raicich, 2015). In addition, tsunami-like waves of meteorological origin – meteotsunamis – may lead to a rise in sea levels of a few tens of centimetres along the open coastline of Istria (Šepić et al., 2015), although these appear mostly during the spring and summer seasons (Vilibić and Šepić, 2009). These cumulative sea levels should be added to wave heights when assessing the worst-case scenario impact of a storm on the coastline in question.

By contrast, there are no significant reported seismic tsunamis in the northern Adriatic Sea over the last two hundred years (Tinti et al., 2004; Maramai et al., 2007; Fago et al., 2014) and the worst-case hazard scenarios provide for a maximum tsunami height no higher than 20 cm (Paulatto et al., 2007; Tiberti et al., 2008). Seismic tsunami waves might impact the deeper southern Adriatic, but are not considered capable of reaching the northern Adriatic Sea, mainly due to substantial reflection on the Palagruža Sill (Sørensen et al., 2012).

3. Materials and methods

3.1. Field and underwater surveys

Field activities were carried out between 2016 and 2018. Beside general geological and geomorphological observations and measurements on the rocks exposed along the investigated coast (lithostratigraphy, depositional and tectonic discontinuities, karst features, marine encrustations and bioerosion), obtained by a common field methodology for a geological research, research was focussed on the boulders inventory, location and measurements. We collected direct measurements related to boulder size and imbrication by means of a measuring tape and a compass. The correct elevations of the boulders were measured by means of an optical-level Wild Heerbrugg Leica NA24. The values were adjusted for the local tide elevation at the time of the survey.

To determine the location and distance from the shoreline of each boulder, aerial-photo interpretations complemented field activities. Distances were measured perpendicular to the coastline, taking into account the boulder imbrication and the geometry of the sloping coast. Boulder sources were identified as large portions – platy or rectangular slabs – that were missing from the sloping coastlines and the coast edge, or isolated submerged boulders in a few cases.

The study has been implemented with data collected during the 2012 snorkel surveys carried out in the frame of the “Geoswim Project”. The latter aimed to collect time-lapse images of all the Istrian coasts while swimming using a mask and fins (Furlani, 2012; Furlani et al., 2014b).

In addition, detailed submerged profiles of the boulder sites were carried out by direct underwater visual observations in the course of the aforementioned Geoswim project and other additional snorkel surveys around the islands close to the study area. A detailed survey of the coast was also carried out by kayak in order to verify the correlation between the submerged limestone features in the nearshore zones (discontinuities, rupture surfaces, detachment scarps, holes), the number and shape of the deposited boulders and the occurrence of fresh impact marks. We used the Sonar Phone Velixar with Navionics maps to reconstruct the bathymetry, useful for calculating the amplification of waves approaching the coast.

3.2. Boulder geomechanical parameters

Boulder shapes were classified using the methodology developed by Blott and Pye (2008). This classification is based on the degree of elongation and flatness using the length ratios of the three block axis.

Boulder densities were calculated by means of the relation provided by Katz et al. (2000), that correlates the density with the Hammer Rebound (HR) index obtained using an N-Type Schmidt Sclerometer (SH) (Viles et al., 2011). HR index is a function of the resistance of surface material to the impact of the sharp tip incorporated in the SH and is used for calculation of rock properties such as intact rock strength (IRS) and density (Yilmaz and Sendir, 2002). We collected 28 non-destructive measurements, according to ISRM recommendations, by pushing the SH far from surfaces where fossils, discontinuities or weathering processes occur and avoiding oblique impacts, as suggested by Aydin and Basu (2005). To obtain more reliable HR results, we discarded the five lower HR values for each boulder, whereas the remaining five were averaged, as suggested by ISRM (1978). The formula developed by Katz et al. (2000) was tested on different types of rocks, including limestones and showed a very good correlation between HR-obtained values and laboratory measured values. The boulder density (ρ) was calculated to the averaged HR value using the equation:

$$\rho = 1308.2Ln(HR) - 2873.9 \quad (1)$$

3.3. Hydrodynamic modelling

To evaluate the minimum wave heights required to detach a boulder from the coast-edge or the nearshore environment, a hydrodynamic approach was adopted. In particular, we applied the well-known and widely used equations developed by Nandasena et al. (2011) and Engel and May (2012) (Table 1). Although taking into account the limits of the hydrodynamic models, as described in the Introduction, we used these equations only to obtain an estimation of the wave heights necessary to detach and transport the boulders, taking into consideration that in this area of the Mediterranean basin, significant tsunami events have not been recorded.

With reference to the analyses of the ERA Interim dataset, that provided the maximum wave height values measured in the Adriatic

Table 1
Hydrodynamic equations (a, b and c for major, medium and minor axis respectively; ρb = boulder density; ρw = sea water density; CL = lift coefficient = 0.178; θ = bed slope angle; μ = coefficient of static friction = 0.65; V = boulder volume; CD = coefficient of drag = 1.95; q = boulder area coefficient = 0.73).

Equation	Joint bounded scenario	Submerged/subaerial scenario (saltation)
Nandasena et al. (2011) Tsunami	$H_T > \frac{0.5\,c*\left(\frac{\rho_b}{\rho_w}-1\right)*(cos\vartheta+\mu sen\vartheta)}{C_L}$	$H_T \geq \frac{0.5\,c*\left(\frac{\rho_b}{\rho_w}-1\right)*cos\vartheta}{C_L}$
Nandasena et al. (2011) Storm	$H_S > \frac{2\,c*\left(\frac{\rho_b}{\rho_w}-1\right)*(cos\vartheta+\mu sen\vartheta)}{C_L}$	$H_S \geq \frac{2\,c*\left(\frac{\rho_b}{\rho_w}-1\right)*cos\vartheta}{C_L}$
Engel and May (2012) Tsunami	$H_T \geq \frac{0.5\,V\,(\rho_b-\rho_w)(cos\vartheta+\mu sen\vartheta)}{C_L\,(a*c*q)\,\rho_w}$	$H_T \geq \frac{0.5\,\mu\,V\,\rho_b}{C_D\,(a*c*q)\,\rho_w}$
Engel and May (2012) Storm	$H_S \geq \frac{2\,V\,(\rho_b-\rho_w)(cos\vartheta+\mu sen\vartheta)}{C_L\,(a*c*q)\,\rho_w}$	$H_S \geq \frac{2\,\mu\,V\,\rho_b}{C_D\,(a*c*q)\,\rho_w}$

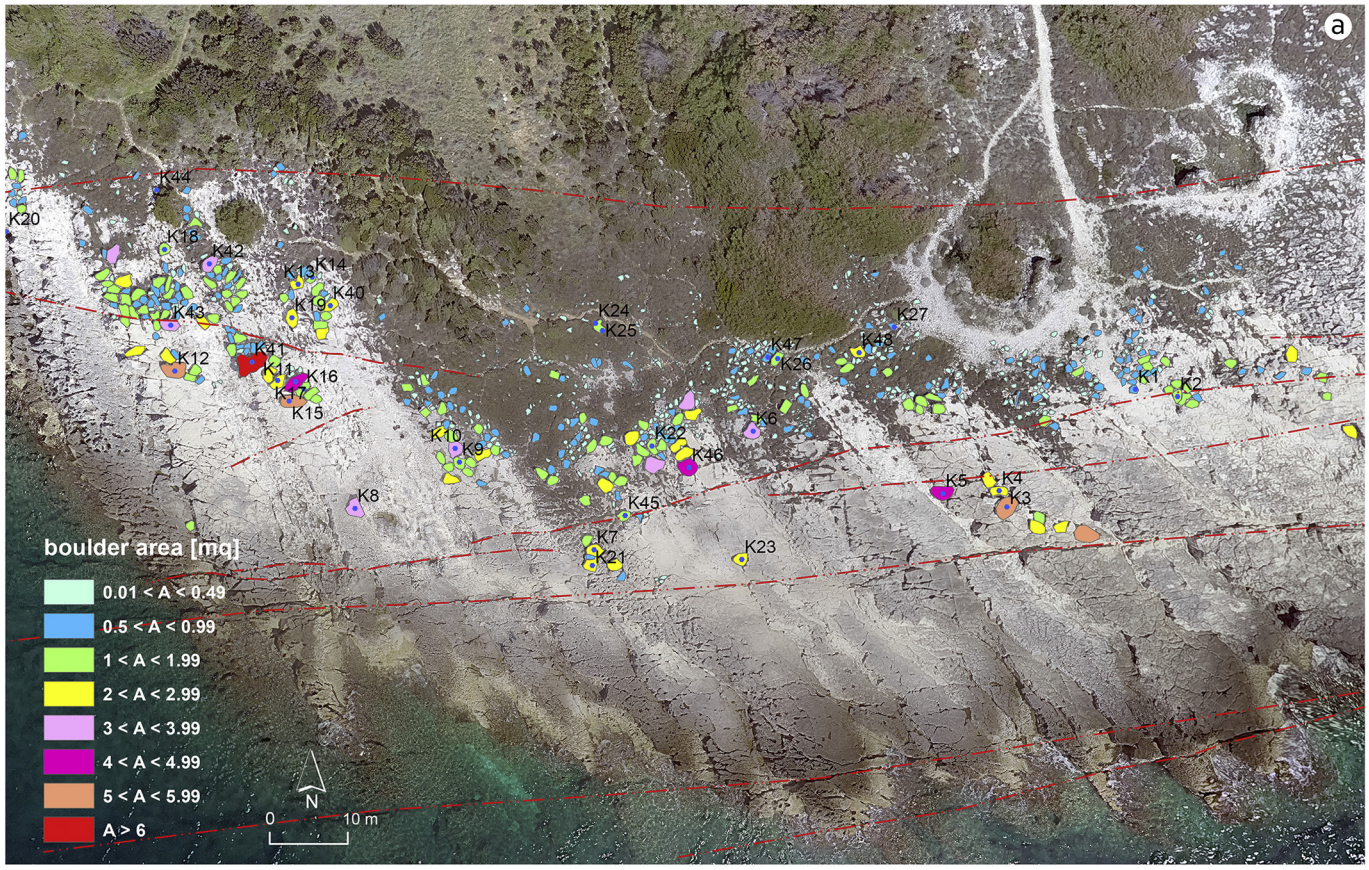

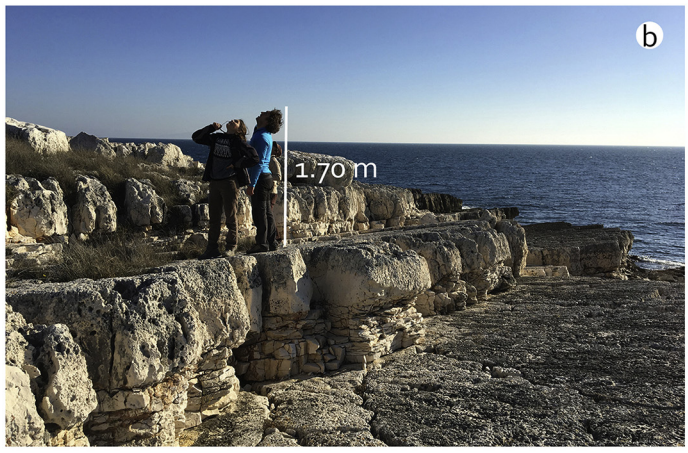

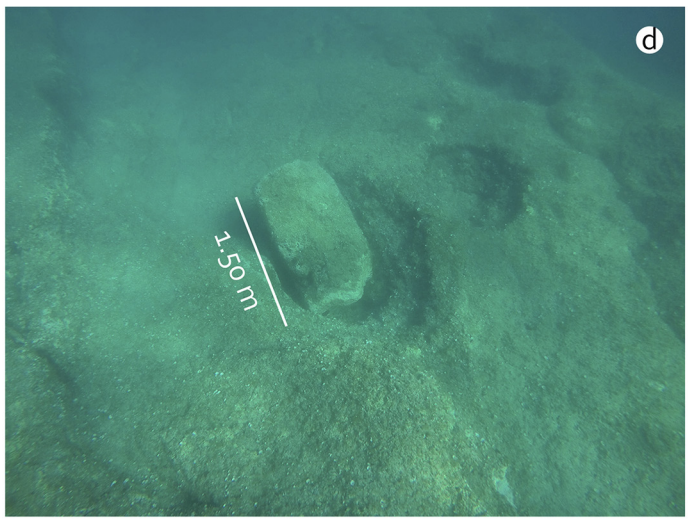

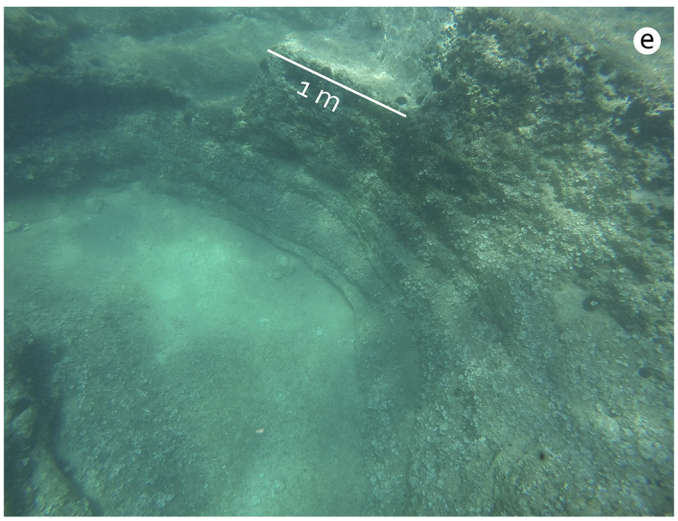

(caption on next page)

Fig. 2. a) View of the boulder deposit of Kamenjak Cape obtained with UAV with the spatial distribution of the selected boulders for analyses and representation of all the boulders as a function of their area (calculated by means of ERSI ArcGis); b) particular of the gentle sloping coast of Kamenjak Cape where thin platy limestone layers favored the erosion and the detachment of large portions of the rocky outcrop; c) the boulders have been lifted and accumulated teens of metres from the coastline; d) isolated submerged boulder; e) fresh and recent detachment scarp.

during long-lasting sirocco events, we applied the Sunamura and Horikawa (1974) equation. The latter is used to evaluate the wave height at breaking point (H_b) of a coastal area in order to estimate possible wave amplification due to the bathymetry:

$$\frac{Hb}{H0} = (tan\,\beta)^{0.2} * \left(\frac{H0}{L0}\right)^{-0.25} \quad (2)$$

where H_b is the breaking wave height, H_0 is the wave height in deep water, β is the slope of the sea bed in the coastal area, and L_0 the wave length in deep water.

3.4. AMS ^{14}C analysis

Radiocarbon age datings on three marine biogenic carbonate encrustations sampled from three different boulders were performed in order to estimate the timeframe of their detachment and transport. These were performed by the CeDaD Laboratory (*Centro di Datazione e Diagnostica* of the University of Salento, Italy). The conventional radiocarbon ages obtained were calibrated by using OxCal Ver. 3.10 software (Reimer et al., 2013). We used the reservoir correction: $\Delta R = 45 \pm 21$ years as the average value for the Mediterranean Sea. Specifically, the calibrated calendar age is obtained by graphic interpolation. This approach intrinsically takes into account both the local and marine reservoir effects.

3.5. Aerial-photo analysis

Aerial-photos were collected both from the Web and by field acquisitions of UAV images. UAVs are widely used in geoscience fields (i.e., Casella et al., 2016, 2017) and offer major benefits from their ability to provide high-resolution photographic images from reduced flight times (Francioni et al., 2018). Digital Photogrammetry (DP) techniques, through the processing of images collected by drones, enabled the reconstruction of high-resolution orthophotos and a Digital Elevation Model (DEM) of a large sector of the coastal area. Two different survey campaigns were carried out in 2016 and 2017 using a UAV equipped with a HD camera. These followed the shoreline at different heights, ranging between 20 m and 60 m. The main purpose of the UAV survey was to monitor the boulder field over time in order to detect displacements that had occurred in the course of the year. In addition, pictures from the UAV were integrated with those collected directly in the field in order to determine accurate boulder axis sizes and, consequently, their volumes. Orthophotos and the DEM reconstructed during the UAV surveys were also compared with the available Google Earth® images (2007, 2009, 2012, 2013, 2016), those of the Geoportal of the State Geodetic Administration of the Republic of Croatia (geoportal.dgu.hr) and the pictures that were collected during the swim surveys carried out within the Geoswim 2012 project along the Istrian coast from 2nd July to 31st July of that year (Furlani et al., 2014b).

3.6. Wave and climate analysis

To understand the weather and ocean processes which might lead to detachment and transport of large boulders, we estimated the climatology of relevant atmospheric (10 m wind speed, and 2 m temperature) and ocean variables (significant wave height - SWH, mean wave direction). Variables were downloaded from the ERA Interim reanalysis dataset for the grid point in front of the Premantura Promontory (44.5°N 14.1°E). The extracted series covered the 1979–2016 period and had a temporal resolution of 6 h. We used the ERA Interim wind and wave product as it is the best available product over decadal timescales that has already been widely used for Adriatic wave studies (e.g., Signell et al., 2005). We further focused our analysis on SWH during sirocco and bora wind conditions, as these are the two winds which generate highest waves in the Adriatic (Smirčić et al., 1996). We defined the sirocco as a wind which blows between due south (180°) and due east (90°), and the bora as a wind blowing from between due north (0°) and due east (90°).

4. Results

4.1. Geological and geomorphological characteristics of the site

The area where limestone boulders are scattered is located along the southern coastal part of the Jugo Promontory (Fig. 1d), mostly between the sea and the vegetated zone. Most of the boulders are exposed along the southwestern coast of Cape Kamenjak (Fig. 2a), which is directly exposed to the sirocco-induced waves. Layer dip direction and dip angles on the southwestern part the Cape Kamenjak are 88/12 (Fig. 1d). An indistinct fracture (joint) system has developed along the bed strike, i.e., generally running North-South (possibly an axial plane cleavage of the Istrian anticline), whereas a distinct opened-fractures system generally strikes East-West (mean dip direction and dipping angle measuring 350/85) as per metre-scale distances. Thus, quadrangular limestone fragments are formed by the fracture network and, together with the bedding planes discontinuities, these boulders are predisposed to detachment. The same system is also visible underwater as well as in potholes with enlarged fractures, pebbles, cobbles and isolated boulders.

The limestone beds are 0.05 m to 1.5 m thick and truncated by the longitudinal (along the strike) and transversal fracture net, along with the scars of previous detachments and abrasion along the shore. Thus, the truncations and discontinuities are oriented towards the strongest impacts of the south-to-southeasterly waves generated by intense south and southeasterly winds, while the limestone fragments are prone to detachment under the hydrodynamic forces that develop during extreme wave events. What is more, the coast slopes gently (10°) towards the sea and in combination with gently inclined limestone beds to the east, (Fig. 2b), form a cascades with relatively smooth and broad ramps on the upper-bedding surfaces elongated along the strike (towards the north), with steep truncations towards the west.

Rudist shell layers and the facies of limestones outcropping along the coast are recognisable in many of the boulders, attesting to their local provenance. Detachment from submerged limestone layers' accounts for at least 20 boulders, which are partially covered by marine biogenic carbonate encrustations formed by coralline algae, serpulids and barnacles and bored by date mussel *Lithophaga lithophaga* and the flask-shell *Rocellaria dubia*. The submerged environment is characterised by a relatively shallow sea bed with a stepped topography where isolated boulders and fresh detachment scarp are visible (Fig. 2d, e). Fresh crush marks are visible on some boulders and on the coastal limestone pavement.

Other boulder deposits have been observed at Stipan and on the surrounding islands of Fenoliga, Ceja and Šekovac (Fig. 1b), in particular during a snorkel survey carried out around the latter islet during the summer of 2016. Two boulder deposits were observed on the Šekovac islet (Fig. 1c), and the southern one is located within the pavement of a quarry dating back to the Roman period (Furlani et al., 2011). This is indicative both for the timing of the deposition (post-Roman

Table 2
The selected boulders: GPS position (WGS84 UTM 33 N Coordinate System), measured elevation above msl, distance from the coastline (perpendicular to wave direction, taking into account boulder imbrication), rock density, mass, volume, a, b and c axis sizes, results of the hydrodynamic equations provided by Nandasena et al. (2011) and Engel and May (2012) and the most appropriated pre-existing scenario (JBS: joint bounded scenario; SAS: subaerial scenario).

Boulder	LAT	LONG	Elevation [m asl]	Distance [m]	Density [g/cm^3]	Mass [t]	Volume [m^3]	a axis [m]	b axis [m]	c axis [m]	Nandasena et al. storm [m]	Nandasena et al. tsunami [m]	Engel & May storm [m]	Engel & May tsunami [m]	Scenario
K01	4,957,610	414,841		45	2.11	1.769	0.84	1.4	1	0.6	7.88	1.97	10.79	2.7	JBS
K02	4,957,610	414,850		38	1.88	4.220	2.24	1.6	1	1.4	14.63	3.66	20.04	5.01	JBS
K03	4,957,600	414,827		37	2.16	15.643	7.23	3.23	1.6	1.4	17.34	4.34	3.1	0.77	SAS
K04	4,957,600	414,826		35	1.74	2.984	1.71	2.2	1.3	0.6	4.68	1.17	2.02	0.51	SAS
K05	4,957,600	414,815	4.25	38	2.02	9.580	4.75	3.3	1.6	0.9	9.72	2.43	2.89	0.72	SAS
K06	4,957,610	414,796	5.95	44	2.19	6.307	2.88	2	1.6	0.9	11.42	2.86	3.14	0.78	SAS
K07	4,957,600	414,770		23	1.81	5.866	3.23	2.1	1.4	1.1	10.56	2.64	14.47	3.62	JBS
K08	4,957,600	414,745	2	27	2.16	7.657	3.54	2.25	1.65	0.95	13.17	3.29	18.05	4.51	JBS
K09	4,957,610	414,749		26	2.13	7.174	3.36	2.8	1.5	0.8	10.79	2.69	14.77	3.69	JBS
K10	4,957,610	414,749		26	2.11	4.928	2.34	2.6	1.5	0.6	7.88	1.97	10.79	2.7	JBS
K11	4,957,620	414,741	3.4	39	1.74	7.325	4.21	2.7	1.3	1.2	10.43	2.61	14.29	3.57	JBS
K12	4,957,620	414,729		34	2.19	11.057	5.05	2.7	1.7	1.1	13.96	3.49	3.33	0.83	SAS
K13	4,957,630	414,739		58	2.13	0.365	0.17	1.07	0.8	0.2	2.69	0.67	3.69	0.92	JBS
K14	4,957,630	414,741		56	2.16	1.873	0.88	1.14	1.4	0.55	7.40	1.85	10.14	2.54	JBS
K15	4,957,620	414,739		34	2.13	3.661	1.72	2.6	1.1	0.6	8.08	2.02	11.06	2.77	JBS
K16	4,957,620	414,739		35	2.12	9.762	4.58	2.2	1.6	1.3	15.70	3.92	3.06	0.76	SAS
K17	4,957,620	414,737		34	2.14	3.770	1.77	1.7	1.35	0.77	10.37	2.52	14.20	3.55	JBS
K18	4,957,630	414,724		47	2.17	2.133	1.00	1	1	1	13.43	3.37	18.44	4.61	JBS
K19	4,957,630	414,730		45	2.15	2.381	1.12	1.55	0.9	0.8	10.77	2.69	14.75	3.69	JBS
K20	4,957,630	414,698		24	2.13	0.821	0.38	1.1	1	0.35	4.72	1.18	6.45	1.61	JBS
K21	4,957,600	414,772		27	2.13	6.691	3.14	2.05	1.7	0.9	10.87	2.72	3.25	0.81	SAS
K22	4,957,600	414,776		45	2.13	3.828	1.79	1.65	1.45	0.75	9.06	2.26	2.77	0.69	SAS
K23	4,957,590	414,790		31	2.14	12.903	6.05	3.6	2.4	0.7	8.45	2.11	4.58	1.15	SAS
K24	4,957,620	414,778		70	2.12	1.690	0.79	1.2	1.1	0.6	7.25	1.81	2.10	0.52	SAS
K25	4,957,620	414,774		69	2.13	2.315	1.08	1.55	1.4	0.5	6.04	1.51	2.67	0.67	SAS
K26	4,957,620	414,793		58	2.16	2.285	1.07	1.7	0.9	0.7	8.45	2.11	1.72	0.43	SAS
K27	4,957,630	414,810		71	2.12	0.806	0.38	1.05	0.6	0.6	7.25	1.81	1.15	0.29	SAS
K28	4,957,670	414,623	5.6	29	2.24	0.353	0.16	1.05	0.6	0.25	3.32	0.83	1.20	0.30	SAS
K29	4,957,640	414,610	3.4	31	2.32	2.002	0.86	1.7	1.45	0.35	4.94	1.23	3.01	0.75	SAS
K30	4,957,660	414,620	5.6	24	2.30	2.223	0.97	1.55	1.25	0.5	6.92	1.73	2.57	0.64	SAS
K31	4,957,640	414,533		80	2.13	2.867	1.34	1.6	1.4	0.6	7.25	1.81	2.67	0.67	SAS
K32	4,957,650	414,614	5	42	2.44	8.571	3.52	2.45	2.05	0.7	10.77	2.69	4.47	1.12	SAS
K33	4,957,580	414,559	4.6	11	2.27	0.731	0.32	2.5	1.4	1	5.42	1.36	1.42	0.36	SAS
K34	4,957,590	414,562	8	26	2.48	1.312	0.53	1.25	1	0.9	7.45	1.86	2.00	0.50	SAS
K35	4,957,600	414,573	8.5	31	2.24	4.781	2.13	2.1	1.45	0.7	9.29	2.32	15.40	3.85	JBS
K40	4,957,620	414,743	4.4	65	2.48	6.672	2.69	1.68	1.6	1	15.86	3.96	24.34	6.09	SAS
K41	4,957,620	414,734	4.9	48	2.19	25.054	11.44	4.4	2.6	1	12.69	3.17	21.41	5.37	SAS
K42	4,957,640	414,729		64	2.16	6.424	2.97	2.7	1.1	1	12.40	3.10	21.22	5.30	SAS
K43	4,957,620	414,722		43	2.27	10.535	4.64	2.55	1.4	1.3	17.63	4.41	28.94	7.24	JBS
K44	4,957,640	414,717	4.9	70	2.08	0.972	0.47	1.3	0.9	0.4	4.58	1.15	8.14	2.04	JBS
K45	4,957,600	414,774	4.25	40	2.22	6.658	3.00	2.1	1.3	1.1	14.28	3.57	23.92	5.90	SAS
K46	4,957,600	414,782		50	2.41	20.774	8.60	3.4	2.3	1.1	16.65	4.16	26.06	6.51	SAS
K47	4,957,620	414,797	7	68	2.16	1.505	0.7	1	0.87	0.8	9.92	2.48	16.97	4.24	SAS
K48	4,957,620	414,803	7.2	70	2.39	1.837	0.77	1.6	0.8	0.6	8.93	2.23	14.08	3.52	SAS

coastal activities) and for the topography of the coastline more suitable for boulder accumulation after its anthropic modification. Some boulders may have been resized by quarrying activities rather than having been detached along natural discontinuity planes.

4.2. Physical properties, elevation and statistics

According to the recent update of traditional Udden-Wentworth grain-size scale for extremely coarse-grained sedimentary particles developed by Terry and Goff (2014), the entire population of clasts can be classified as boulders (clasts between 0.25 and 4.1 m). A total of about 950 boulders were identified using orthophotos obtained by means of UAV image processing (Fig. 2a). Of these, 44 were selected for the analysis and measurement. Table 2 lists the position, field measurements (sizes, elevation and distance from the coastline) and the outputs of geomechanical activities (density).

The maximum length of axis does not exceed 4.4 m and is often around 1 m in length. Intermediate axes vary from a minimum of 0.6 m to 2.4 m; most of the minimum axes do not exceed 1 m.

Boulder density varies from 1.74 to 2.19 g/cm^3 (Table 2).

Fig. 3 shows the shapes of the selected 44 boulders using the methodology developed by Blott and Pye (2008). Flat boulders and elongate boulders make up > 50% of the total and are dominant with respect to equidimensional boulders such as equant and sub-equant boulders. Conversely, blade boulders make up 15% while plate and rod areas are not populated.

Mass and distance from the coastline were plotted in a graph (Fig. 4), which shows that 73% of the boulders analysed were transported inland at distances from the coastline varying from 20 m to 50 m. Moreover, a clear relationship between mass and distance from the coast was observed: boulders with a mass exceeding 10 t stop at a maximum distance of 50 m, whereas boulders with a lighter weight may reach 70–80 m inland, as shown by a cluster of 5 boulders at a distance of 70 m.

The boulders accumulated at the greatest distances from the coast represent the maximum inundation reached by the waves.

Fig. 4 shows also that the boulder shape does not have a crucial role in transport mechanisms. For boulders exceeding 50 m of distance from

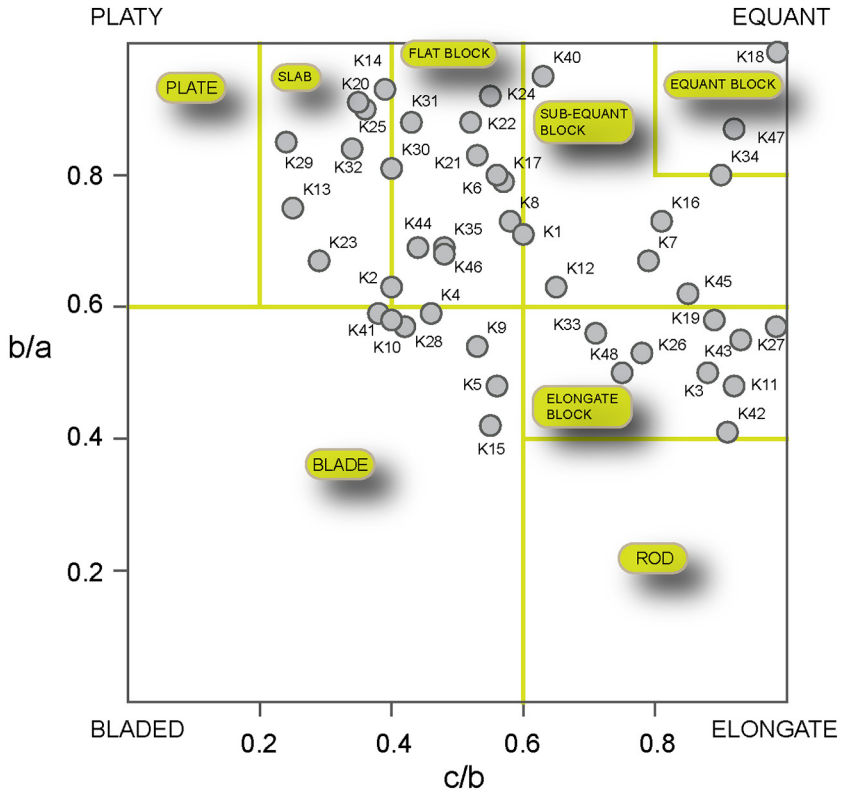

Fig. 3. Boulders shapes plotted in the Zingg diagram according to classification developed by Blott and Pye (2008).

the coast, the ratio between equidimensional boulders (red dots)/ number of boulders is 2/11. The latter is approximately the same value (9/44) when considering the ratio on the total population.

Our attention was particularly focused on a 7 t boulder (K8), characterised by a peculiar orange colour on its surface due to karst weathering (Fig. 5). The elevation of the boulder is 2 m above sea level. It is 27 m from the coastline and is oriented by a longer axis facing the main wave direction. Its isolated position and intense orange colour allowed us to identify the boulder easily using aerial and terrestrial images.

The K8 boulder (Fig. 5a; Table 2) is characterised by intact sub-recent biogenic carbonate encrustations a few centimetres thick on the southern and upper sides (Fig. 5b), mainly produced by coralline algae and serpulids as well as by more fragile barnacle shells. Noteworthy is an absence of sub-recent encrustations or borings on either its western or northern side (Fig. 5c). On the eastern side there are only solitary barnacle shells and rare bivalves along with some serpulid tubes (Fig. 5d). The encrusted surfaces are heavily bored by date mussels and flask-shells (Fig. 5e), especially the southern face, where some holes contain intact date mussel shells up to 10 cm long.

4.3. Model results

First of all, the most likely setting (submerged or subaerial joint-bounded scenario) prior to transportation and the type of movement (sliding, rolling, saltation) were determined for each boulder (Table 2).

Estimated storm wave heights for the selected boulders (Table 2) using the Nandasena et al. (2011) model vary from a few metres to the maximum value of 17.63 m for boulder K43, which is located 43 m from the coastline. As suggested by Piscitelli et al. (2017), the results

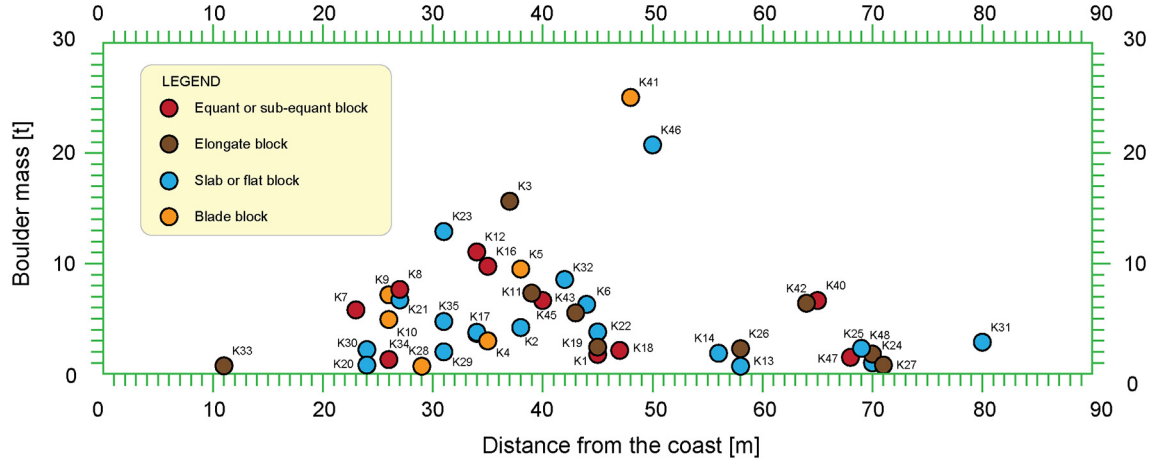

Fig. 4. Relationship between the distance from the coast (x) and the boulder mass (y). The boulders are represented as a function of their shape.

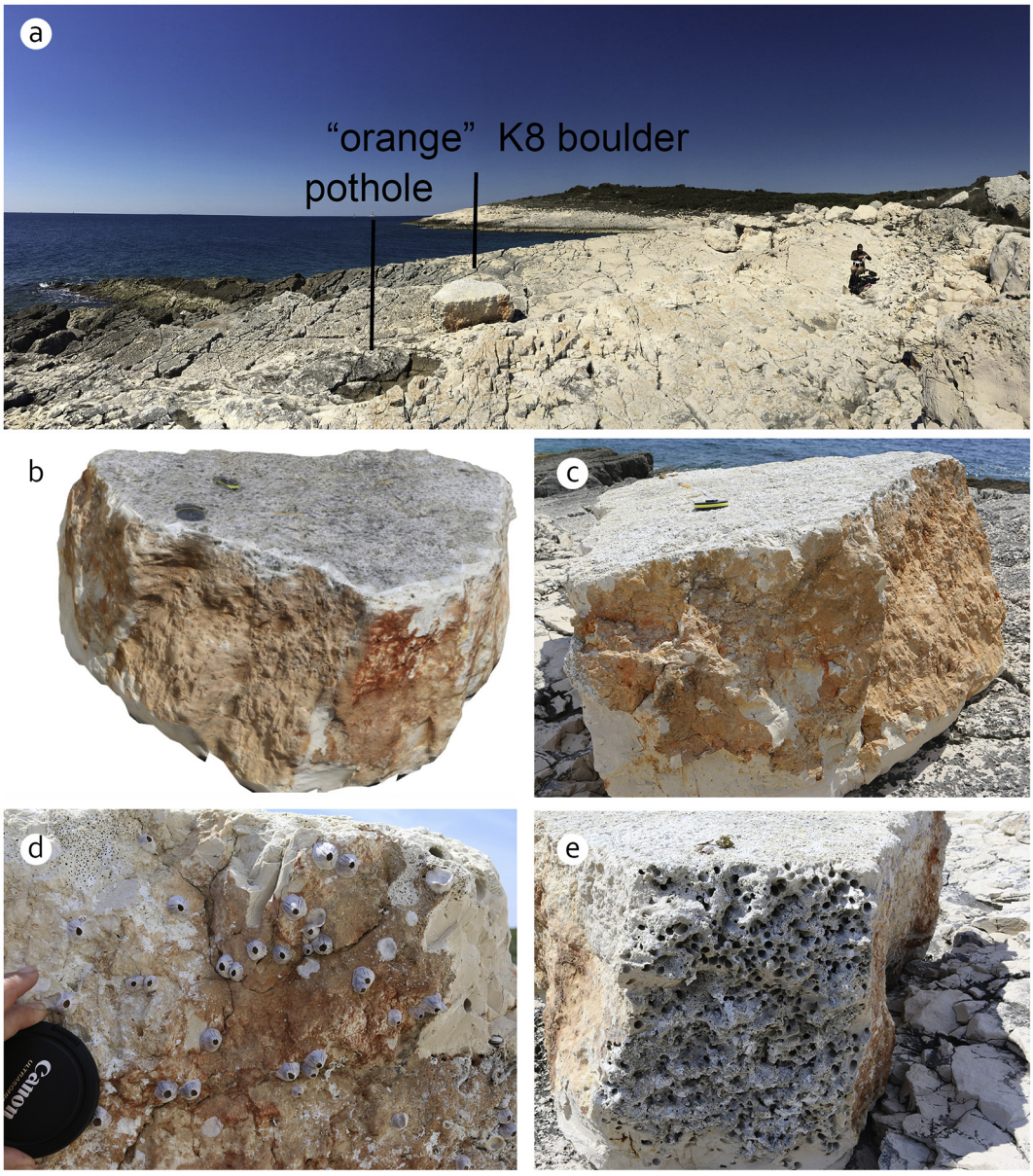

Fig. 5. K8 boulder: a) aerial view of the deposit; b) SFM 3D reconstruction; c) orange northwest-exposed side of the boulder; d) barnacle shells; e) south-exposed side of the boulder with thick encrustation and Lithophaga borings.

obtained using the Engel and May (2012) model overestimate the wave heights required: also with this model K43 boulder obtained the maximum value, but with an estimated wave height of ~29 m.

The detachment of the K8 boulder required a storm wave height of about 13 m according to the Nandasena model and about 18 m using the Engel and May model. Conversely, the calculated tsunami wave heights are too high and not comparable to those measured during historically-documented events (Tiberti et al., 2008).

4.4. Radiocarbon datings

Three marine organisms sampled from biogenic carbonate encrustations of K17, K43 and K44 boulders were dated (Table 3). Radiocarbon datings on samples collected on the K17 and K43 gave back values post-1955 CE. Conversely, the date mussel sampled from K44 boulder, the furthest from the coastline, provided a time emersion ranging between 1447 and 1525 CE.

4.5. UAV and digital photogrammetric analysis

The photogrammetric analysis was applied mainly to evaluate the movements of K8. Thanks to its isolated position, its orange colour related to weathering processes and the nearby presence of a dark, shallow pothole, it is clearly recognisable on satellite images.

The results of the comparison of images allowed us to hypothesize the arrival of K8 as being obviously post-late 2012 (after July, because it was not observed during the Geoswim 2012 survey around the Istrian coastline) and probably between late 2013 (not present in Google Earth image) and the spring of 2014, when it became clearly visible in the Croatian Geoportal image (Fig. 6).

The other boulders remained in their initial position, although the resolution of the satellite images is limited.

A comparison of the orthophotos reconstructed in 2016 and 2017 with the UAV survey shows no evidence of movement within the boulder field.

Table 3
^{14}C AMS datings of marine organisms performed by the CeDaD Laboratory (Centro di Datazione e Diagnostica) of the University of Salento, Brindisi, Italy.

Sample	Species	Radiocarbon Age (BP) or pMC (Percent Modern Carbon)	δ^{13}C (‰)	Calibrated age(AD)	Note
LTL18581A K17	*Serpulidae*	112.74 ± 0.45 pMC	−0.4 ± 0.5		after 1955 CE
LTL18582A K43	*Serpulidae*	104.18 ± 0.45 pMC	5.4 ± 0.4		after 1955 CE
LTL18583A K44	*Lithophaga lithophaga*	874 ± 45 BP	6.7 ± 0.5	1447–1525 CE	

5. Impact of local weather conditions

The time series of the number of days per year in which SWH was larger than its 99 percentile value are plotted in Fig. 7a. On average we found 3.65 days with extreme waves per year and of these 3.01 related to a bora wind, 0.48 to a sirocco, and 0.16 to other winds. There is a significant ($p < 0.05$) positive trend of 3.3 days/50 years of extreme waves per year, and a significant ($p < 0.05$) positive trend of 2.8 days/50 years of extreme waves per year during bora conditions. Trends related to sirocco are not significant. As for extreme years, 2012 clearly jumps out from the data set as the year with the maximum number of days with extremely high waves (10.6 days), with most of them

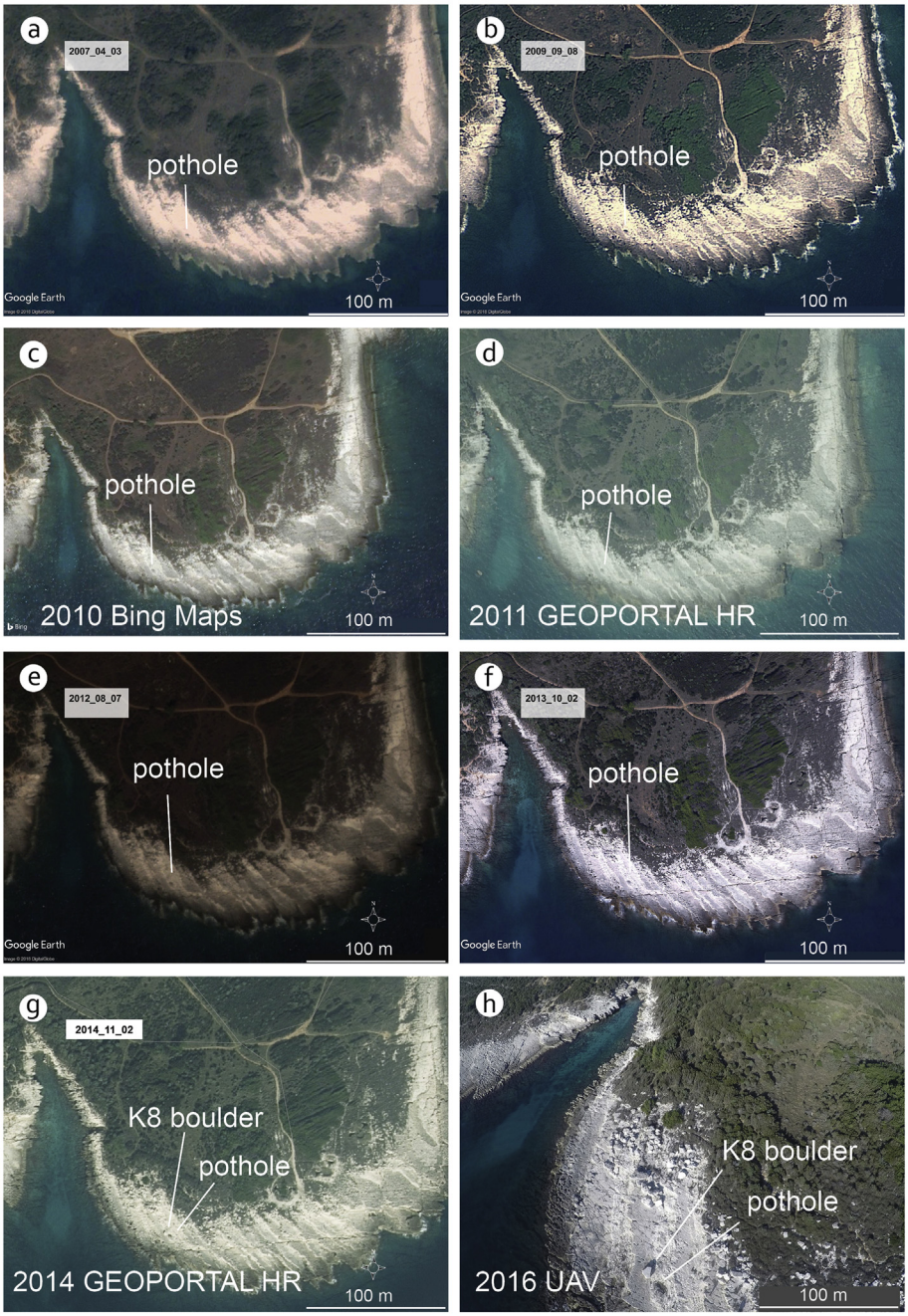

Fig. 6. Comparison between Google Earth (a, b, e, f), Bing Maps (c), the Croatian Geoportal (d, g) and 2016 UAV (h) aerial photos where both the large pothole and K8 are clearly visible.

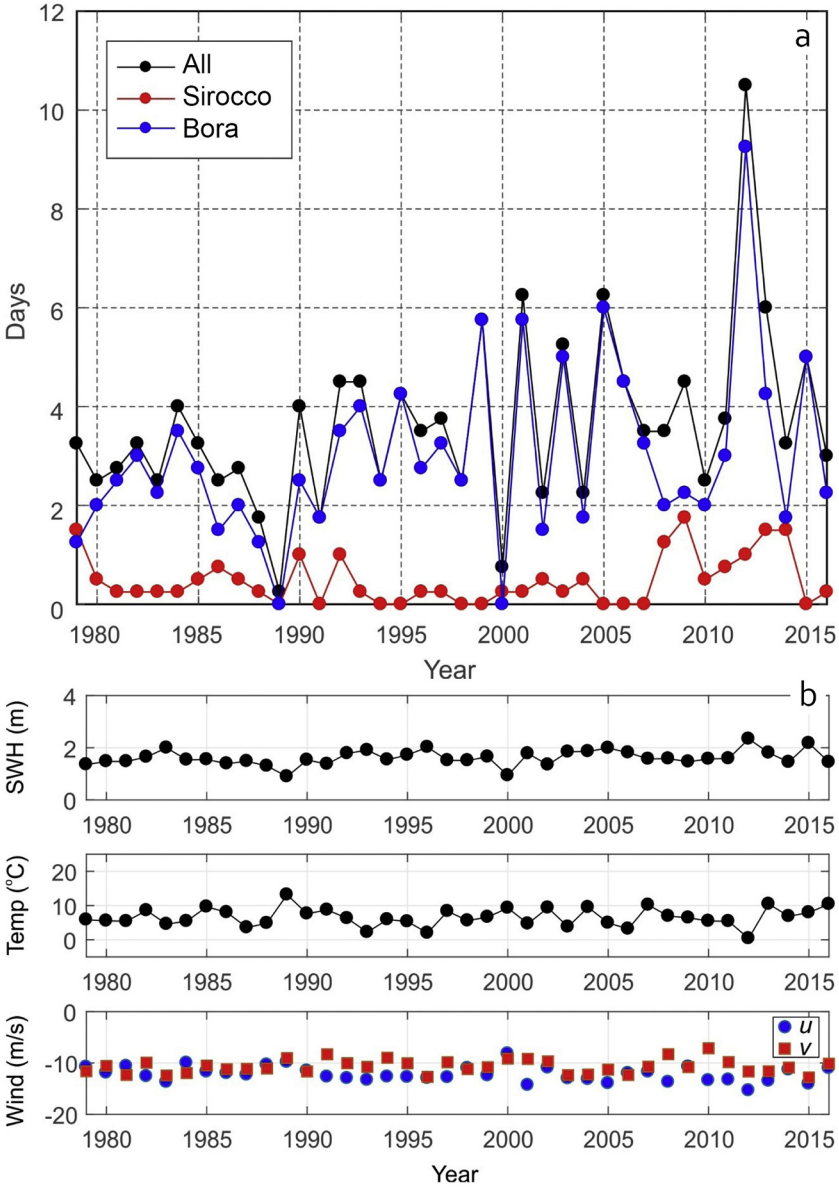

Fig. 7. a) Number of days per year in which significant wave height was larger than 99 percentile of the whole time series, separately for: entire time series, bora wind conditions, and sirocco wind conditions, all for the grid point southeast of Premantura Promontory (44.5°N 14.1°E) from the ERA Interim dataset; b) Average values of significant wave height (SWH), air temperature and wind direction components (u eastward, v northward; oceanographic convention) estimated for 10 strongest wintertime (December through February) bora events during the Interim period (1979–2016). Bora wind is defined as the wind blowing from the north (0°) to the east (90°).

modelled to appear under bora conditions. This number is almost three times higher than the average, and much higher than the number of days with extreme waves for the following ranked years (2001 and 2005, with 6.2 days each, and 2013 with 6.0 days).

Two discrepancies between the model and the observations/measurements should be noted here: (i) the highest waves in the Adriatic do not appear during the bora, but during sirocco wind events (Smirčić et al., 1996), and (ii) the wave heights estimated by the ECMWF represent underestimates by at least 20–30% when compared to the actual measurements (Cavaleri and Bertotti, 1997). To understand these discrepancies better, we looked at the most extreme waves measured during the period 1978–1986 at gas extraction platforms offshore from the Premantura Promontory (Smirčić et al., 1996). The highest bora-induced waves were measured on 8th January 1981, with maximum wave height of 7.2 m, and a maximum SWH of 3.9 m. In quite a similar fashion, the modelled ECMWF maximum SWH for the given date for approximate location of Ivana platform (~50 km W from Premantura Promontory) was 3.9 m. On the contrary, the highest sirocco induced waves were measured on 22nd December 1979, with maximum wave height of 10.2 m, and maximum SWH of 7.3 m, whereas the maximum ECMWF modelled SWH for this event was 3.5 m, less than half of the measured SWH. Nevertheless, the ECMWH SWH of 3.5 m is still close to the 99.75th percentile (3.5 m) of the entire ECMWF SWH time series at a location closest to the position of the Ivana platform. These analyses imply that the ECMWF wave data is representative of strong bora events, both in terms of the timing and modelled wave heights. However, for sirocco events, the maximum modelled wave heights appear at the correct time but are strongly underestimated.

There are two relevant weather and coastal processes which might lead to the detachment and transportation of boulders along the eastern coast of the northern Adriatic. The first process is related to extreme bora, and second to extreme sirocco events. During strong bora events, short but steep ocean waves are generated over the limited fetch of the area's coastal channels. Together with sea spray, these ocean waves hit the coastlines causing wetting and salting of exposed limestones (Fig. 7b). When this process is accompanied by prolonged air temperatures below 0 °C, the frosting of wetted and salted cracks in the limestones (so called frost and salt mechanism, cf. Robinson and Jerwood, 1987) may occur, causing a crumbling of the limestone, and detachment of large emergent boulders from the ground. This, in particular, may be a mechanism that explains the detachment of subaerial boulders at some distance from the sea, as bora-generated sea spray can

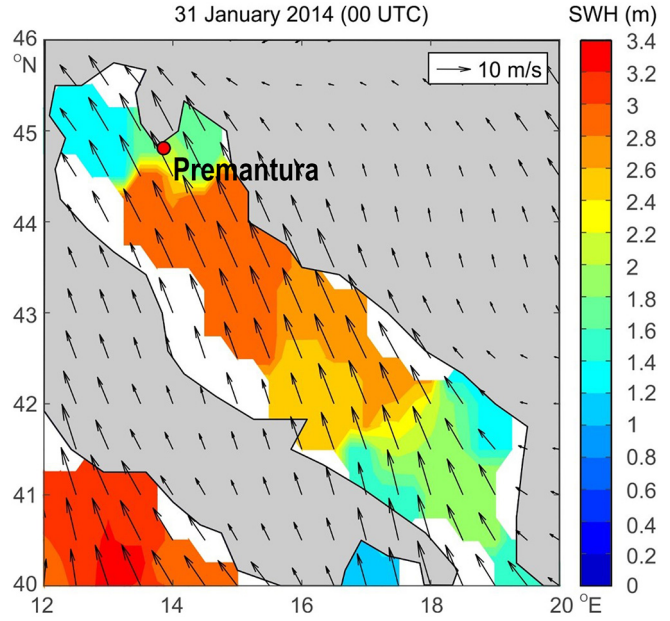

Fig. 8. Significant wave height (SWH) and 10-m wind fields over the Adriatic Sea on 31 January 2014 (00 UTC). Fields are extracted from the ERA Interim dataset. Premantura Promontory is marked with a red dot. (For interpretation of the references to colour in this figure legend, the reader is referred to the web version of this article.)

easily be transported over distances of O(100 m) to the land, i.e. to positions of the boulders in question (Table 2) (Grisogono and Belušić, 2009).

The most recent period during which bora driven detachment processes could have occurred is the winter of 2011/2012 (Fig. 8) on which extensive bibliographic data have been published (e.g., Mihanović et al., 2013; Davolio et al., 2015). This extreme bora event started around 25th January 2012 and lasted until 14th February 2012, with three major peaks in the bora reaching speeds above 50 m/s in the coastal region and channels. At the Rijeka climatological station (located 70 km northeast of Premantura), nine and three days between 2nd and 12nd February 2012 were classified as extremely cold and with record-breaking cold temperatures, respectively, with maximum temperatures below 0 °C (MHS, 2012; 2013). Extensive sea spray conditions were documented throughout the coastal area, including the Premantura Promontory. Since the K8 boulder appeared on the photos after early 2014, it is apparent that it was not transported to its present position during the winter of 2011/2012. However, it is possible that its initial partial detachment happened precisely during this winter, and, furthermore, that some of other subaerial boulders were detached from the limestone during this winter.

As far as the sirocco is concerned, the marine waves generated by this wind have a much longer period and are higher (the maxima of observed wavelength and height being 156.13 m and 10.2 m, respectively) than the bora generated waves (the maxima of observed wavelength and wave height being 65.97 m and 7.20 m, respectively) (Smirčić et al., 1996), and, furthermore, are directed towards tip of the Premantura Promontory (as opposed to the bora waves which are directed towards the Italian coast). Such waves could have detached submerged boulders from the limestone by shear mechanical force, and given that they are high enough and long enough, these marine waves may have also carried boulders ashore (Table 2).

Since the K8 boulder was clearly submerged before it was transported onshore, it is most likely that its final detachment from the limestone and its transportation to the present location were due to sirocco-induced ocean waves. The ECMWF data reveals that during the approximate period of K8's appearance on the shore (sometimes during late 2013 – early 2014) the highest sirocco-generated waves at Premantura Promontory occurred during the storm of 30th January – 2nd February 2014 (Fig. 8). This storm and related waves peaked on 31st January, when a sirocco wind blew across the entire Adriatic, resembling the synoptic situation of 22nd December 1979 during which greatest wave heights were measured (Leder et al., 1998). The maximum modelled SWH at location of a gas extraction platform during 30th January – 2nd February 2014 was 2.9 m, implying that real SWH at this location could have been higher than 6 m. Maximum wave height is generally estimated to be up to 75% higher than SWH (Wiegel, 1961), so in this case it could have been higher than 10.6 m. Closer to the shore, at location of the Premantura Promontory, the waves could have been even higher due to the amplification caused by the bathymetry. From the Eq. (2), assuming that $H0 = 10.6$ m, $L0 = 150$ m, $\beta = 0.1875$ m, we can estimate the wave height at breaking point to $HB = 14.7$ m, which is within the theoretical heights of waves needed to transport K8 to its present location according to Nandasena (13.173 m) and Engel storm (18.046 m) estimates. In addition, the surge of 1.25 m above mean sea level was reported in the northern Adriatic (Venice), peaking precisely on 31st January 2014 (https://www.mosevenezia.eu/my-product/acqua-alta-gennaio-2014-2/). The surge can be linked to the extreme wave conditions driven by the Adriatic-wide sirocco wind (De Zolt et al., 2006), adding approximately 0.5–1 m to their height. No other extreme wave events related to sirocco storms of comparative force were estimated for the winter of 2013/2014.

6. Discussion

The data collected at the Premantura site allowed us to identify a coastal deposit of limestone boulders in the northern Adriatic Sea for the first time, which until now had been considered a low energy, semi-enclosed basin.

6.1. Geomorphology and rock mechanics

The site holds approximately 950 boulders ranging in volume from 0.1 m^3 to 11.5 m^3. The majority are situated between 11 m and 80 m from the coastline and are in some areas lie one on top of another or scattered in clusters at elevations ranging between 2 m and 8.5 m above sea level. Some boulders have maintained a clear imbrication towards the south-east.

The rocky coast is composed of alternating thick- and thin-bedded limestone gently inclined towards the sea. The beds are constant in orientation and act as a natural ramp for the drifting, rolling and saltation of boulders during the transport and accumulation processes. Relatively smooth and broad ramps on the upper-bedding surfaces, that are elongated along the strike (towards the north) have allowed extreme waves to move the boulders to the north during multiple events, while some of the rocks in question have probably also rolled down to the next cascade along the steep western scarps. Thus, their distribution makes it look as if these boulders have been conveyed there, although there is a clear relation with the morphology of the boulder field described (see Results). What is more, the smooth, flat upper bedding surfaces also allow for the greatest propagation of extreme waves that have accumulated the boulders on top of the ramps, along the boundary of the rocky shore with the vegetated zone (Fig. 2a).

Boulder sizes are predisposed by the interplay of the regular bedding and a dense fracture pattern. Kennedy et al. (2017) observed during a typhoon in the Philippines that the shape has a role in boulders transport: non-rectangular cross-sections tend to be transported more easily than those with rectangular cross-sections. Conversely, we observed that the mass has a crucial role in transport process: boulders not exceeding 10 t can reach distances over 50 m whereas the different types of shapes classified according to the methodology developed by Terry and Goff (2014) have not influence on the spatial distribution.

The fracturing of the rock masses, which is governed by rock type as well as the existence and orientation of faults and joints, is exploited and enhanced by repeated wave action (Herterich et al., 2018). By coincidence, the rocky coast at Premantura is composed of stratified layers of differing degrees of hardness due to the occurrence of alternate limestone beds with small spacing. Over long timescales, the softer layers have been gradually eroded away, quarrying boulders that can fracture under their own weight (and consequently be moved onto the coast) either due to frost and salt weathering or as a result of waves or wave impact. Herterich et al. (2018) modelled the hydraulic fracture of rocks from cliffs and shore platforms due to wave run-up and demonstrated that the bending stress induced by loading during crack filling or impact can create and/or propagate microcracks in the rock to complete its fracture and detachment. At the Premantura Promontory, the repeated action of wave pressure against the fractures and the limestone beds has detached boulders from the bedrock.

6.2. Biological marine carbonate encrustations

The rupture surface can be both subaerial and submarine, with a subaerial predominance, as testified by the widespread karren landforms that occur both on the boulders and on the limestone beds. Conversely, there are dozens of boulders, lying at even greater distances from the coastline, which include biological marine carbonate encrustations, including a few very fresh ones, attesting to their marine provenance from a submerged environment. The latter is characterised by the occurrence of fresh detachment scarps, isolated boulders on the sea bottom and the sockets observed during the snorkel surveys (Fig. 2). In addition, fresh crush marks are visible on some boulders and on the coast, implying rolling and saltation as a transport mechanism.

One of the most distant boulders from the coastline (K44, 70 m), dated using radiocarbon dating performed on an encrusted date mussel, seems to have been transported onto dry land between 1447 and 1525 CE. The other two dated boulders provided recent dates, out of the range of radiocarbon (post-1955 CE). These dates suggest that erosion of the Premantura Promontory rocky coast was active during recent centuries (or even before) and that the boulder field is the result of multiple historical and recent extreme storm events, although they are insufficient to explain the accumulation of all the boulders. However, as suggested by Rixhon et al. (2018), radiocarbon ages of boring bivalves, such as the studied sample, because of post-mortem carbonate dissolution, recrystallization and replacement, may overestimate the age of the emersion from the sea.

6.3. The K8 boulder

One of the largest boulders is the K8 (2.25 × 1.65 × 0.95 m, 7.657 t) which is characterised by an abundance of fresh encrustations produced by marine organisms (barnacles, oysters, Bryozoa, serpulids and vermetids) as well as by the boring bivalves, date mussels and flask-shells. The non-encrusted western and northern sides of K8 are probably the boulder's detachment surfaces. As the southern side of K8 is characterised by the most extensive and the deepest borings and this was the side that probably originally faced the open sea or at least did so for some decades (Peharda et al., 2015) before the boulder was deposited. The general orientation (y) of K8 is probably its original one or rotated ~90° counter-clockwise. It means that the boulder was drifted by extremely powerful southerly waves of > 13 m of height towards the north (Table 2). There is no damage on its encrusted surfaces of the sort that would be present had it been subject to rolling. The presence of predominantly solitary barnacle shells, known to be the earliest colonisers of marine substrates (Henschel et al., 1990), suggests that the eastern side (possibly originally eastern or southern if rotated ~90° counter-clockwise) probably detached along the most recent fracture. This, in turn, suggests that a previous detachment event in the same locality probably happened a few months or a year before.

The comparison between satellite images, UAV ortophotos and pictures collected during the Geoswim 2012 snorkelling surveys along the coast of Istria (Furlani, 2012; Furlani et al., 2014b) and from the web shows that K8 was transported to its current position during a severe storm that occurred between late 2013 and early 2014. In this period no tsunami occurred in the Adriatic Sea. A major storm with gale-force sirocco wind jumps out as the most likely generative force for the detachment and movement of this boulder. This storm, which peaked on 31st January 2014, affected the entire Adriatic Sea, i.e. the sirocco wind blew across the whole Adriatic, resembling the synoptic situations in which highest wave heights were observed (Leder et al., 1998).

6.4. Wave height model

The application of the hydrodynamic equations provided by Nandasena et al. (2011) and Engel and May (2012), chosen for a particular scenario and type of movement, provided height values for storm waves that are acceptable for the local waves during severe storms and in particular to storms related to southeasterly winds. Inshore, favourable bathymetric conditions can produce the amplification and deformation of an incoming storm waves by as much as several metres higher than maximum offshore waves, particularly for extreme waves, which have wavelengths comparable to the sea depth. Conversely, the values obtained for a tsunami origin of the beached boulders are too high if compared to what was observed during the past in this area of the Adriatic Sea.

The estimated maximum wave heights at Premantura Promontory were ~14.75 m, which is, according to Nandasena's theory, sufficient to transport boulders ashore. We hypothesize that boulders are detached by frost and salt mechanisms during severe bora conditions, in particular during those situations in which the bora wind is linked to air temperatures below 0 °C. Short, steep bora waves and associated sea spray fill cracks within limestone with water, which then freezes due to low temperatures. The freezing and subsequent thawing can cause further cracking and eventually detachment of limestone fragments. The most recent year in which this process could have occurred was the cold winter of 2011/2012. Then, the boulders are carried onshore during sirocco events when much longer and higher waves are generated. We estimate that sirocco generated waves can have wave heights up to ~15 m at the location of the Premantura Promontory, which is enough to transport most of boulders observed to their present day location, according to Nandasena's storm theory (Table 2).

Although the northern Adriatic Sea can be considered as a semi-closed and sheltered basin, the large boulders in our study demonstrate that storm waves and related sea spray can reach high elevations and inundate/spray the coastal sector to significant heights. In particular, the peculiarity of the Premantura Promontory in terms of its topographical and geomorphological setting and its exposure towards the south and southeast, with major sirocco waves coming from the southern sectors, and major bora waves (and related sea spray) coming from the eastern and northern sectors, explains detachment, transportation and accumulation of these boulders.

If the arrival of boulder K8 was reconstructed by means of satellite images, wave data and hydrodynamic models, the deposition of the remaining boulders can be ascribed to multiple past extreme wave events, even stronger than the 2014 one. We hypothesize that the boulder detachment mechanism was more effective during the past, when the coastal slope was intact and the boulders were progressively removed and thrown onto the upper storm berm that represents the maximum inundation limit reached by the boulders (Fig. 2a). Through the centuries the coast has been eroded through the removal of rocky material and has been shaped forming channels delimited by scarps that acted as ramps for boulder movements. These ramps are now almost like polished floors, lying between the sea level and about 45 m from the coast, where boulders, mostly isolated, may be displaced under the

action of waves and backwash, or arrive for the first time following recent storm waves (as in the case of K8). In fact, the underwater environment shows very few fresh detachment scarps and one of them could be that left by the K8 boulder. By contrast, the more distant accumulations seem stable, suggesting that after deposition, no further and stronger events have reached such elevations.

The mechanism may also have been favored over the centuries by slow sea level rise inundating new portions of the rocky coast, bringing the action of seawater in the form of tides and normal waves into contact with limestone beds that were previously stable, in a subaerial environment, causing their resizing and rupture. The occurrence of exceptional severe events, such as the severe bora event of 2012 and the strong sirocco storm of early 2014, may have caused their quarrying and detachment.

7. Conclusions

This paper presents an analysis of the first reported coastal boulder deposit in the northern Adriatic Sea.

To examine the mechanism of detachment, transport and accumulation of the boulders, we carried out a geological and geomorphological field survey, UAV and digital photogrammetric analyses and hydrodynamic equations calibrated on underwater bathymetric profiles. The study site is located at Premantura (in the south of Istria) on a promontory where the topography, together with the bedding planes and a dense joint pattern, favour the mechanisms promoting detachment. Most of the boulders originated in a subaerial environment, as testified by the widespread karren landforms that occur both on the boulders and on the limestone beds. Conversely, the occurrence of biogenic marine encrustations on dozens of the boulders bears witness to their infra or sublittoral origin. We hypothesize that the bora-induced sea-spray, and subsequent water freezing and thawing – a mechanism that can cause limestone to break - were responsible for detachment of the subaerial boulders now lying far from the shoreline. Conversely, sirocco-induced storm waves were responsible for detachment of boulders from both emerged and submerged environments and their subsequent movement ashore.

Using available meteorological data that report maximum wave heights of 10.8 m during severe sirocco storms, the wave height at the breaking point has been estimated at about 15 m due to the amplification caused by the local topography of the sea bed. Therefore, storm waves would have had the necessary energy to detach and transport all the boulders for which the minimum required wave heights needed for transport are < 15 m (Table 2).

Comparisons between satellite images from 2008 to 2017, pictures collected from the Internet, pictures collected during snorkel surveys along the coast during the summer of 2012 and UAV images taken in 2016 and 2017 allowed us to identify the emplacement of at least one new boulder (K8) with an estimated weight of 7.65 tons during late 2013 or early 2014.

These results are supported by an analysis of a strong storm event (the sirocco storm of 30th January to 2nd February 2014) which occurred within the possible time range of the appearance of this boulder and that could be responsible for it. Considering that some of the previously submerged boulders of similar weight to the K8 boulder are located further from the coast than the K8 boulder, we may conclude that even more extreme weather conditions and higher waves may have occurred during previous events in the area.

The main reasons why a tsunami origin was excluded for the analysed boulders are the climate and physical issues of the study area (strong winds, severe winter conditions, strong sirocco waves and a favourable exposure of the coast to sirocco-generated waves, an intense bedding and joint pattern of limestones and a very suitable natural rocky pavement for boulder transport) together with the absence of any reported record of significant recent or historical tsunami event. Despite the limits to the application of the hydrodynamic equations, the storm wave results obtained are comparable with local wave data while tsunami wave heights are too high, even if compared with the recorded values.

The novelty of this paper is the occurrence of such rocky coastal boulders (taking into account their sizes, weights and distribution on the coast) in this part of the Mediterranean basin – the relatively shallow northern Adriatic Sea, which is considered as a semi-enclosed basin - and the finding of a realistic connection with a severe and powerful storm event for the emplacement of at least one boulder that, a few years ago, was somewhere beneath the sea.

Acknowledgements

This work was carried out within the framework of the Geoswim Project (Resp. Stefano Furlani, University of Trieste), MOPP–Medflood INQUA-CMP 1603 Project and of the Croatian Science Foundation projects GEOSEKVA (Grant IP-2016-06-1854) and ADIOS (Grant IP-2016-06-1955). ECMWF ERA Interim dataset is available at https://www.ecmwf.int/en/forecasts/datasets/archive-datasets/reanalysis-datasets/era-interim. The Authors are grateful to Ms. Nicole Briones and Ms. Nicole Foucher of the University of Andres Bello, Vina del Mar, Conception, Santiago, to Dr. Chiara Boccali and Enrico Zavagno of the University of Trieste as well as friends Diego Manna, Rodolfo Riccamboni and Martina Zaccariotto for the very precious field support. Special thanks are due to the Falck family for their financial support.

References

Antonioli, F., Ferranti, L., Fontana, A., Amorosi, A., Bondesan, A., Braitenberg, C., Dutton, A., Fontolan, G., Furlani, S., Lambeck, K., Mastronuzzi, G., Monaco, C., Spada, G., Stocchi, P., 2009. Holocene relative sea-level changes and vertical movements along the Italian and Istrian coastlines. Quat. Int. 206, 102–133.

Autret, R., Dodet, G., Fichaut, B., Suanez, S., David, L., Leckler, F., Ardhuin, L., Ammann, J., Grandjean, P., Allemand, P., Filipot, J.-F., 2016. A comprehensive hydro-geomorphic study of cliff-top storm deposits on Banneg Island during winter 2013–2014. Mar. Geol. 382, 37–55.

Aydin, A., Basu, A., 2005. The Schmidt hammer in rock material characterization. Eng. Geol. 81, 1–14.

Barbano, M.S., Pirrotta, C., Gerardi, F., 2010. Large boulders along the south-eastern Ionian coast of Sicily: storm or tsunami deposits? Mar. Geol. 275, 140–154.

Benner, R., Browne, T., Bruckner, H., Kelletat, D., Scheffers, A., 2010. Boulder transport by waves: progress in physical modeling. Z. Geomorphol. 54 (Suppl. 3), 127–146.

Biolchi, S., Furlani, S., Antonioli, F., Baldassini, N., Deguara, J., Devoto, S., Di Stefano, A., Evans, J., Gambin, T., Gauci, R., Mastronuzzi, G., Monaco, C., Scicchitano, G., 2016. Boulder accumulations related to extreme wave events on the eastern coast of Malta. Nat. Hazards Earth Syst. Sci. 16, 737–756.

Blott, S.J., Pye, K., 2008. Particle shape: a review and new methods of characterization and classification. Sedimentology 55, 31–63.

Carbognin, L., Teatini, P., Tomasin, A., Tosi, L., 2010. Global change and relative sea level rise at Venice: what impact in term of flooding. Clim. Dyn. 35, 1055–1063.

Casella, E., Rovere, A., Pedroncini, A., Stark, C.P., Casella, M., Ferrari, M., Firpo, M., 2016. Drones as tools for monitoring beach topography changes in the Ligurian Sea (NW Mediterranean). Geo-Mar. Lett. 36, 151–163.

Casella, E., Collin, A., Harris, D., Ferse, S., Bejarano, S., Parravicini, V., Hench, J.L., Rovere, A., 2017. Mapping coral reefs using consumer-grade drones and structure from motion photogrammetry techniques. Coral Reefs 36 (1), 269–275.

Causon Deguara, J., Gauci, R., 2017. Evidence of extreme wave events from boulder deposits on the south-east coast of Malta (Central Mediterranean). Nat. Hazards 86 (Suppl. 2), 543–568.

Cavaleri, L., Bertotti, L., 1997. Search of the correct wind and wave fields in a minor basin. Mon. Weather Rev. 125, 1964–1975.

Cerovečki, I., Orlić, M., Hendershott, M.C., 1997. Adriatic seiche decay and energy loss to the Mediterranean. Deep-Sea Res. I 44, 2007–2029.

Davolio, S., Stocchi, P., Benetazzo, A., Bohm, E., Riminucci, F., Ravaioli, M., Li, X.-M., Carniel, S., 2015. Exceptional Bora outbreak in winter 2012: Validation and analysis of high-resolution atmospheric model simulations in the northern Adriatic area. Dyn. Atmos. Oceans 71, 1–20.

De Zolt, S., Lionello, P., Nuhu, A., Tomasin, A., 2006. The disastrous storm of 4 November 1966 on Italy. Nat. Hazards Earth Syst. Sci. 6, 861–879.

Engel, M., May, S.M., 2012. Bonaire's boulder fields revisited: evidence for Holocene tsunami impact on the Leeward Antilles. Quat. Sci. Rev. 54, 126–141.

Engel, M., Oetjen, J., May, S.M., Brückner, H., 2016. Tsunami deposits of the Caribbean – towards an improved coastal hazard assessment. Earth Sci. Rev. 163, 260–296.

Etienne, S., Paris, R., 2010. Boulder accumulations related to storms on the south coast of the Reykjanes Peninsula (Iceland). Geomorphology 114, 55–70.

Fago, P., Pignatelli, A., Piscitelli, A., Milella, M., Venerito, M., Sansò, P., Mastronuzzi, G., 2014. WebGIS for Italian tsunami: a useful tool for coastal planners. Mar. Geol. 35,

369–376.
Fichaut, B., Suanez, S., 2011. Quarrying, transport and deposition of cliff-top storm deposits during extreme events: Banneg Island, Brittany. Mar. Geol. 283, 36–55.
Francioni, M., Salvini, R., Stead, D., Coggan, J., 2018. Improvements in the integration of remote sensing and rock slope modeling and rock slope modelling. Nat. Hazards 90, 975–1004.
Furlani, S., 2012. The Geoswim project: snorkel-surveying along 250 km of the Southern and Western Istrian Coast. Alpine Mediterr. Quat. 25 (2), 7–9 (ISSN: 22797327).
Furlani, S., Biolchi, S., Auriemma, R., Tunis, G., Cucchi, F., Antonioli, F., 2011. New archaeological and geomorphological markers along the istrian coasts (Croatia) and their relations with relative sea-level changes. Alpine Mediterr. Quat. 24, 35–37 (ISSN: 22797327).
Furlani, S., Cucchi, F., Biolchi, S., 2012. Late Holocene widening of karst voids by marine processes in partially submerged coastal caves (Northeastern Adriatic Sea). Geogr. Fis. Din. Quat. 35, 129–140. ISSN: 03919838. https://doi.org/10.4461/GFDQ.2012.35.12.
Furlani, S., Pappalardo, M., Gomez-Pujol, L., Chelli, A., 2014a. The rocky coasts of the Mediterranean and Black Sea. In: Kennedy, D.M., Stephenson, W.J., Naylor, L.A. (Eds.), Rock Coast Geomorphology: A Global Synthesis. Geological Society Memoir, London 40(1). pp. 89–123.
Furlani, S., Ninfo, A., Zavagno, E., Paganini, P., Zini, L., Biolchi, S., Antonioli, F., Coren, F., Cucchi, F., 2014b. Submerged notches in Istria and the Gulf of Trieste: results from the Geoswim Project. Quat. Int. 332, 37–47.
Goto, K., Miyagi, K., Kawamata, H., Imamura, F., 2010. Discrimination of boulders deposited by tsunamis and storm waves at Ishigaki Island, Japan. Mar. Geol. 269, 34–45.
Grisogono, B., Belušić, D., 2009. A review of recent advances in understanding the meso- and microscale properties of the severe Bora wind. Tellus A 61, 1–16.
Gušić, I., Jelaska, V., 1990. Stratigrafija gornjokrednih naslaga otoka Brača u okviru geodinamske evolucije Jadranske karbonatne platforme (Upper Cretaceous stratigraphy of the Island of Brač within the geodynamic evolution of the Adriatic carbonate platform). Djela Jugoslavenske akademije znanosti i umjetnosti, 69, Institut za geološka istraživanja, OOUR za geologiju. (160 pp., Zagreb).
Hearty, P.J., 1997. Boulder deposits from large waves during the last interglaciation on North Eleuthera, Bahamas. Quat. Res. 48, 326–338.
Hearty, P.J., Tormey, B.R., 2017. Sea-level change and superstorms; geologic evidence from the last interglacial (MIS 5e) in the Bahamas and Bermuda offers ominous prospects for a warming Earth. Mar. Geol. 390, 347–365.
Heimann, D., 2001. A model-based wind climatology of the eastern Adriatic coast. Meteorol. Z. 10, 5–16.
Henschel, J.R., Cook, P.A., Branch, G.M., 1990. The colonization of artificial substrata by marine sessile organisms in False Bay. 1. Community development. S. Afr. J. Mar. Sci. 9 (1), 289–297.
Herterich, J.G., Cox, R., Dias, F., 2018. How does wave impact generate large boulders? Modelling hydraulic fracture of cliffs and shore platforms. Mar. Geol. 399, 34–46.
Imamura, F., Goto, K., Ohkubo, S., 2008. A numerical model for the transport of a boulder by tsunami. J. Geophys. Res. Oceans 113, CO1008. https://doi.org/10.1029/2007JC004170.
ISRM, 1978. Suggested methods for determining hardness and abrasiveness of rocks. Int. J. Rock Mech. Min. Sci. Geomech. Abstr. 15, 89–97.
Jurkovšek, B., Biolchi, S., Furlani, S., Kolar-Jurkovšek, T., Zini, L., Jež, J., Tunis, G., Bavec, M., Cucchi, F., 2016. Geology of the Classical Karst Region (SW Slovenia–NE Italy). J. Maps 12, 352–362.
Katz, O., Reches, Z., Roegiers, J.C., 2000. Evaluation of mechanical rock properties using a Schmidt Hammer. Int. J. Rock Mech. Min. Sci. 37, 723–728.
Kennedy, A.B., Mori, N., Yasuda, T., Shimozono, T., Tomiczek, T., Donahue, A., Shimura, T., Imai, Y., 2017. Extreme block and boulder transport along a cliffed coastline (Calicoan Island, Philippines) during Super Typhoon Haiyan. Mar. Geol. 383, 65–77.
Korbar, T., 2009. Orogenic evolution of the External Dinarides in the NE Adriatic region: a model constrained by tectonostratigraphy of Upper cretaceous to Paleogene carbonates. Earth Sci. Rev. 96, 296–312.
Kuzmić, M., Grisogono, B., Li, X.M., Lehner, S., 2015. Examining deep and shallow Adriatic bora events. Q. J. R. Meteorol. Soc. 141, 3434–3438.
Lau, A.Y.A., Terry, J.P., Ziegler, A.D., Switzer, A.D., Lee, Y., Etienne, S., 2016. Understanding the history of extreme wave events in the Tuamotu Archipelago of French Polynesia from large carbonate boulders on Makemo Atoll, with implications for future threats in the central South Pacific. Mar. Geol. 380, 174–190.
Leder, N., Smirčić, A., Vilibić, I., 1998. Extreme values of surface wave heights in the Northern Adriatic. Geofizika 15, 1–13.
Maouche, S., Morhange, C., Meghraoui, M., 2009. Large boulder accumulation on the Algerian coast evidence tsunami events in the western Mediterranean. Mar. Geol. 262, 96–104.
Maramai, A., Graziani, L., Tinti, S., 2007. Investigation on tsunami effects in the Central Adriatic Sea during the last century—a contribution. Nat. Hazards Earth Syst. Sci. 7, 15–19.
Marriner, N., Kaniewski, D., Morhange, C., Flaux, C., Giaime, M., Vacchi, M., Goff, J., 2017. Tsunamis in the geological record: making waves with a cautionary tale from the Mediterranean. Sci. Adv. 3 (10), e1700485. https://doi.org/10.1126/sciadv.1700485.
Mastronuzzi, G., Sansò, P., 2004. Large boulder accumulations by extreme waves along the Adriatic coast of Southern Apulia (Italy). Quat. Int. 120, 173–184.
Mastronuzzi, G., Pignatelli, C., Sansò, P., 2006. Boulder fields: a valuable morphological indicator of palaeotsunami in the Mediterranean Sea. Z. Geomorphol. 146, 173–194.
Mastronuzzi, G., Pignatelli, C., Sansò, P., Selleri, G., 2007. Boulder accumulations produced by the 20th February, 1743 tsunami along the coast of Southeastern Salento (Apulia region, Italy). Mar. Geol. 242, 191–205.
Matičec, D., Vlahović, I., Velić, I., Tišljar, J., 1996. Eocene limestone overlying lower cretaceous deposits of Western Istria (Croatia): did some parts of present Istria form land during the cretaceous? Geologia Croatica 49 (1), 117–127.
Međugorac, I., Pasarić, M., Orlić, M., 2015. Severe flooding along the eastern Adriatic coast: the case of 1 December 2008. Ocean Dyn. 65, 817–830.
MHS, 2012. Meteorological and Hydrological Bilten for February 2012. Meteorological and Hydrological Service, Zagreb(60 pp., https://radar.dhz.hr/~stars2/bilten/2012/bilten0212.pdf, accessed 27 August 2018).
MHS, 2013. Meteorological and Hydrological Bilten for November 2013. Meteorological and Hydrological Service, Zagreb(49 pp., https://radar.dhz.hr/~stars2/bilten/2012/bilten1113.pdf, accessed 27 August 2018).
Mihanović, H., Vilibić, I., Carniel, S., Tudor, M., Russo, A., Bergamasco, A., Bubić, N., Ljubešić, Z., Viličić, D., Boldrin, A., Malačič, V., Celio, M., Comici, C., Raicich, F., 2013. Exceptional dense water formation on the Adriatic shelf in the winter of 2012. Ocean Sci. 9, 561–572.
Morton, R.A., Gelfenbaum, G., Jaffe, B.E., 2007. Physical criteria for distinguishing sandy tsunami and storm deposits using modern examples. Sediment. Geol. 200, 184–207.
Morton, R.A., Gelfenbaum, G., Buckley, M.L., Richmond, B.M., 2011. Geological effects and implications of the 2010 tsunami along the central coast of Chile. Sediment. Geol. 242 (1–4), 34–51.
Mottershead, D., Bray, M., Soar, P., Farres, P.J., 2014. Extreme waves events in the central Mediterranean: Geomorphic evidence of tsunami on the Maltese Islands. Z. Geomorphol. 58, 385–411.
Nandasena, N.A.K., Paris, R., Tanaka, N., 2011. Reassessment of hydrodynamic equations: Minimum flow velocity to initiate boulder transport by high energy events (storms, tsunamis). Mar. Geol. 281, 70–84.
Naylor, L.A., Stephenson, W.J., Smith, H.C.M., Way, O., Mendelssohn, J., Cowley, A., 2016. Geomorphological control on boulder transport and coastal erosion before, during and after an extreme extra-tropical cyclone. Earth Surf. Process. Landf. 41, 685–700.
Noormets, R., Crook, K.A.W., Felton, E.A., 2004. Sedimentology of rocky shorelines: 3. Hydrodynamics of megaclast emplacement and transport on a shore platform, Oahu, Hawaii. Sediment. Geol. 172, 41–65.
Nott, J.F., 1997. Extremely high-energy wave deposits inside the Great Barrier Reef, Australia: determining the cause-tsunami or tropical cyclone. Mar. Geol. 141, 193–207.
Nott, J.F., 2003. Waves, coastal boulder deposits and the importance of the pre-transport setting. Earth Planet. Sci. Lett. 210, 269–276.
Öğretmen, N., Cosentino, D., Gliozzi, E., Cipollari, P., Iadanza, A., Yildirim, C., 2015. Tsunami hazard in the Eastern Mediterranean: geological evidence from the Anatolian coastal area (Silifke, southern Turkey). Nat. Hazards 73 (3), 1569–1589.
Paulatto, M., Pinat, T., Romanelli, F., 2007. Tsunami hazard scenarios in the Adriatic Sea domain. Nat. Hazards Earth Syst. Sci. 7, 309–325.
Peharda, M., Puljas, S., Chauvaud, L., Schöne, B.R., Ezgeta-Balić, D., Thébault, J., 2015. Growth and longevity of Lithophaga lithophaga: what can we learn from shell structure and stable isotope composition? Mar. Biol. 162, 1531–1540.
Pepe, F., Corradino, M., Parrino, N., Besio, G., Lo Presti, V., Renda, P., Calcagnile, L., Quarta, G., Sulli, A., Antonioli, F., 2018. Boulder coastal deposits at Favignana Island rocky coast (Sicily, Italy): Litho-structural and hydrodynamic control. Geomorphology 303, 191–209.
Pethick, J., 1984. An Introduction to Coastal Geomorphology. Hodder Arnold Publication (257 pp).
Pignatelli, C., Sansò, P., Mastronuzzi, G., 2009. Evaluation of tsunami flooding using geomorphologic evidence. Mar. Geol. 260, 6–18.
Piscitelli, A., Milella, M., Hippolyte, J.-C., Shah-Hosseini, M., Morhange, C., Mastronuzzi, G., 2017. Numerical approach to the study of coastal boulders: the case of Martigues, Marseille, France. Quat. Int. 439, 52–64.
Polšak, A., 1967. Osnovna geološka karta SFRJ, list Pula, 1:100.000, L33-112 (Basic geological map of SFRY: Sheet Pula L33-112). Instit. za geol. istraž., Zagreb, Savezni geološki zavod, Beograd, 1967.
Pomaro, A., Cavaleri, L., Lionello, P., 2017. Climatology and trends of the Adriatic Sea wind waves: analysis of a 37-year long instrumental data set. Int. J. Climatol. 37, 4237–4250.
Raicich, F., 2015. Long-term variability of storm surge frequency in the Venice Lagoon: an update thanks to 18th century sea level observations. Nat. Hazards Earth Syst. Sci. 15, 527–535.
Raji, O., Dezileau, L., Von Grafenstein, U., Niazi, S., Snoussi, M., Martinez, P., 2015. Extreme sea events during the last millennium in the northeast of Morocco. Nat. Hazards Earth Syst. Sci. 15, 203–211.
Reicherter, K., Becker-Heidmann, P., 2009. Tsunami deposits in the western Mediterranean: remains of the 1522 Almería earthquake? Geol. Soc. Spec. Publ. 316, 217–235.
Reimer, P.J., Bard, E., Bayliss, A., Beck, J.W., Blackwell, P.G, Bronk Ramsey, C., Buck, C.E., Cheng, H., Edwards, R.L., Friedrich, M., Grootes, P.M., Guilderson, T.P., Haflidason, H., Hajdas, I., Hatté, C., Heaton, T.J., Hogg, A.G., Hughen, K.A., Kaiser, K.F., Kromer, B., Manning, S.W., Niu, M., Reimer, R.W., Richards, D.A., Scott, E.M., Southon, J.R., Turney, C., van der Plicht, J., 2013. IntCal13 and MARINE13 radiocarbon age calibration curves 0-50000 years cal BP. Radiocarbon 55 (4). https://doi.org/10.2458/azu_js_rc.55.16947.
Rixhon, G., May, S.M., Engel, M., Mechernich, S., Schroeder-Ritzrau, A., Frank, N., Fohlmeister, J., Boulvain, F., Dunai, T., Brückner, H., 2018. Multiple dating approach (14C, 230^{Th}/U and 36Cl) of tsunami-transported reef-top boulders on Bonaire (leeward Antilles) – current achievements and challenges. Mar. Geol. 396, 100–113.
Robinson, D.A., Jerwood, L.C., 1987. Sub-aerial weathering of chalk shore platforms during harsh winters in southeast England. Mar. Geol. 77, 1–14.
Rodríguez-Ramírez, A., Villarías-Robles, J.J.R., Pérez-Asensio, J.N., Santos, A., Morales,

J.A., Pérez, S.C., León, Á., Santos-Arévalo, F.J., 2016. Geomorphological record of extreme wave events during Roman times in the Guadalquivir estuary (Gulf of Cadiz, SW Spain): an archaeological and paleogeographical approach. Geomorphology 261, 103–118.
Roig-Munar, F.X., Lleonard, R.M., Rodríguez-Perea, A., Martín-Prieto, J.Á., Vilaplana, J.M., Ferrer, B.G., 2017. Propuesta de lugares de interés geológico asociados a bloques y cordones de origen tsunamítico en la costa SE de Menorca (Baleares) - Proposed Geosites for tsunamitic blocks and ridges in the SE coast of Menorca (Baleares). Rev. Soc. Geol. Esp. 30 (1), 31–40.
Scheffers, A., Scheffers, S., 2007. Tsunami deposits on the coastline of west Crete (Greece). Earth Planet. Sci. Lett. 259 (3–4), 613–624.
Scicchitano, G., Monaco, C., Tortorici, L., 2007. Large boulder deposits by tsunami waves along the Ionian coast of South-eastern Sicily (Italy). Mar. Geol. 238, 75–91.
Scicchitano, G., Pignatelli, C., Spampinato, C.R., Piscitelli, A., Milella, M., Monaco, C., Mastronuzzi, G., 2012. Terrestrial Laser Scanner techniques in the assessment of tsunami impact on the Maddalena peninsula (South-eastern Sicily, Italy). Earth Planets Space 64, 889–903.
Šepić, J., Vilibić, I., Fine, I., 2015. Northern Adriatic meteorological tsunamis: Assessment of their potential through ocean modeling experiments. J. Geophys. Res. Oceans 120, 2993–3010.
Shah-Hosseini, M., Saleem, A., Mahmoud, A.-M.A., Morhange, C., 2016. Coastal boulder deposits attesting to large wave impacts on the Mediterranean coast of Egypt. Nat. Hazards 83, 849–865.
Signell, R.P., Carniel, S., Cavaleri, L., Chiggiato, J., Doyle, J.D., Pullen, J., Sclavo, M., 2005. Assessment of wind quality for oceanographic modelling in semi-enclosed basins. J. Mar. Syst. 53, 217–233.
Smirčić, A., Gačić, M., Dadić, V., 1996. Ecological study of gas fields in the northern Adriatic, 3. Surface waves. Acta Adriat. 37, 17–34.
Sørensen, M.B., Spada, M., Babeyko, A., Wiemer, S., Grünthal, G., 2012. Probabilistic tsunami hazard in the Mediterranean Sea. J. Geophys. Res. 117, B01305. https://doi.org/10.1029/2010JB008169.
Soria, J.L.A., Switzer, A.D., Pilarczyk, J.E., Siringan, F.P., Khan, N.S., Fritz, H.M., 2017. Typhoon Haiyan overwash sediments from Leyte Gulf coastlines show local spatial variations with hybrid storm and tsunami signatures. Sediment. Geol. 358, 121–138.
Soria, J.L.A., Switzer, A.D., Pilarczyk, J.E., Tang, H., Weiss, R., Siringan, F., Manglicmot, M., Gallentes, A., Lau, A.Y.A., Yee Lin Cheong, A., Wei Ling Koh, T., 2018. Surf beat-induced overwash during Typhoon Haiyan deposited two distinct sediment assemblages on the carbonate coast of Hernani, Samar, central Philippines. Mar. Geol. 396, 215–230.
Sunamura, T., Horikawa, K., 1974. Two dimensional beach transformation due to waves. In: Proceedings 14th Coastal Engineering Conference. American Society of Civilian Engineers, pp. 920–938.
Surić, M., Korbar, T., Juračić, M., 2014. Tectonic constraints on the late Pleistocene-Holocene relative sea-level change along the north-eastern Adriatic coast (Croatia). Geomorphology 220, 93–103.
Switzer, A.D., Burston, J.M., 2010. Competing mechanisms for boulder deposition on the southeast Australian coast. Geomorphology 114 (1–2), 42–54.
Terry, J.P., Goff, J., 2014. Megaclasts: proposed revised nomenclature at the coarse end of the Udden-Wentworth grain-size scale for sedimentary particles. J. Sediment. Res. 84, 192–197.
Tiberti, M.M., Lorito, S., Basili, R., Kastelić, V., Piatanesi, A., Valensise, G., 2008. Scenarios of earthquake-generated tsunamis for the Italian coast of the Adriatic Sea. Pure Appl. Geophys. 165, 2117–2142.
Tinti, S., Maramai, A., Graziani, L., 2004. The new catalogue of Italian Tsunamis. Nat. Hazards 33, 439–465.
Tsimplis, M.N., Proctor, R., Flather, R., 1995. A two-dimensional tidal model for the Mediterranean Sea. J. Geophys. Res. 100, 16223–16239.
Vacchi, M., Rovere, A., Zouros, N., Firpo, M., 2012. Assessing enigmatic boulder deposits in NE Aegean Sea: importance of historical sources as tool to support hydrodynamic equations. Nat. Hazards Earth Syst. Sci. 12, 1109–1118.
Viles, H., Goudie, A.S., Grab, S., Lalley, J., 2011. The use of the Schmidt Hammer and Equotip for rock hardness assessment in geomorphology and heritage science: a comparative analysis. Earth Surf. Process. Landf. 36, 320–333.
Vilibić, I., 2006. The role of the fundamental seiche in the Adriatic coastal floods. Cont. Shelf Res. 26, 206–216.
Vilibić, I., Šepić, J., 2009. Destructive meteotsunamis along the eastern Adriatic coast: Overview. Phys. Chem. Earth 34, 904–917.
Vlahović, I., Tišljar, J., Velić, I., Matičec, D., Skelton, P.W., Korbar, T., Fuček, L., 2003. Main events recorded in the sedimentary succession of the adriatic carbonate platform from the Oxfordian to the Upper Santonian in Istria (Croatia). In: Vlahović, I., Tišljar, J. (Eds.), Evolution of Depositional Environments from the Palaeozoic to the Quaternary in the Karst Dinarides and Pannonian Basin. 22nd IAS Meeting of Sedimentology, Opatija – September 17–19, 2003, Field Trip Guidebook. pp. 19–56 (Zagreb).
Vlahović, I., Tišljar, J., Velić, I., Matičec, D., 2005. Evolution of the adriatic carbonate platform: palaeogeography, main events and depositional dynamics. Palaeogeogr. Palaeoclimatol. Palaeoecol. 220 (3-4), 333–360.
Watanabe, M., Goto, K., Imamura, F., Hongo, C., 2016. Numerical identification of tsunami boulders and estimation of local tsunami size at Ibaruma reef of Ishigaki Island, Japan. Island Arc 25 (5), 316–322.
Weiss, R., Diplas, P., 2015. Untangling boulder dislodgment in storms and tsunamis: is it possible with simple theories? Geochem. Geophys. Geosyst. 16 (3), 890–898.
Wiegel, R.L., 1961. Wind waves and swell. In: Proc. Seventh Conf. on Coastal Engineering, the Hague, Netherlands, the Engineering Foundation, Council on Wave Research. pp. 1–40.
Williams, D.M., Hall, A.M., 2004. Cliff-top megaclast deposits of Ireland, a record of extreme waves in the North Atlantic-storms or tsunamis? Mar. Geol. 206, 101–117.
Yilmaz, I., Sendir, H., 2002. Correlation of Schmidt hardness with unconfined compressive strength and Young's modulus in gypsum from Sivas (Turkey). Eng. Geol. 66, 211–219.
Zainali, A., Weiss, R., 2015. Boulder dislodgement and transport by solitary waves: Insights from three-dimensional numerical simulations. Geophys. Res. Lett. 42 (11), 4490–4497.